Geophysical Journal International

Geophys. J. Int. (2019) **216,** 1648–1664
Advance Access publication 2018 December 13
GJI Marine geosciences and applied geophysics

doi: 10.1093/gji/ggy524

Traveltime approximation for strongly anisotropic media using the homotopy analysis method

Xingguo Huang[1] and Stewart Greenhalgh[2]

[1]*Department of Earth Science, University of Bergen, P.O. Box* 7803, 5020 *Bergen, Norway. E-mail: xingguo.huang19@gmail.com*
[2]*Department of Geosciences, King Fahd University of Petroleum and Minerals, Dhahran 31261, Saudi Arabia*

Accepted 2018 December 12. Received 2018 June 8; in original form 2018 November 15

SUMMARY

Traveltime approximation plays an important role in seismic data processing, for example, anisotropic parameter estimation and seismic imaging. By exploiting seismic traveltimes, it is possible to improve the accuracy of anisotropic parameter estimation and the resolution of seismic imaging. Conventionally, the traveltime approximations in anisotropic media are obtained by expanding the anisotropic eikonal equation in terms of the anisotropic parameters and the elliptically anisotropic eikonal equation based on perturbation theory. Such an expansion assumes a small perturbation and weak anisotropy. In a realistic medium, however, the assumption of small perturbation likely breaks down. We present a retrieved zero-order deformation equation that creates a map from the anisotropic eikonal equation to a linearized partial differential equation system based on the homotopy analysis method. By choosing the linear and nonlinear operators in the retrieved zero-order deformation equation, we develop new traveltime approximations that allow us to compute the traveltimes for a medium of arbitrarily strength anisotropy. A comparison of the traveltimes and their errors from the homotopy analysis method and from the perturbation method suggests that the traveltime approximations provide a more reliable result in strongly anisotropic media.

Key words: Non-linear differential equations; Seismic anisotropy; Wave propagation.

INTRODUCTION

Seismic anisotropy can arise due to various geological situations such as crystal orientation (Musgrave 1970), parallel cracked rocks (Crampin 1984), sedimentation near salt domes and thin layering in the subsurface (Schoenberg 1983; Tsvankin 1997, 2012). It is important for seismic exploration and investigations of the Earth's interior to recognize the anisotropy. One of the most common and effective approximations to an anisotropic subsurface is the transversely isotropic medium. Modelling seismic traveltimes is clearly essential for understanding and quantification of the kinematic properties of the propagating waves in such media. It finds many applications such as velocity analysis, anisotropic parameter estimation (Alkhalifah 2011a), traveltime tomography (Chapman & Pratt 1992; Zelt & Barton 1998; Zhou *et al.* 2008; Bai & Greenhalgh 2005), seismic migration (Huang *et al.* 2016a; Huang & Sun 2018) and full waveform inversion (Alkhalifah & Choi 2014; Silva *et al.* 2016). The seismic traveltimes can be obtained by solving the nonlinear partial differential equation under the high-frequency assumption; this is referred to as the eikonal equation.

There are several approaches to solve the eikonal equation, such as ray-tracing methods (see e.g. Červenỳ 1972, 2001; Červenỳ & Pšenčík 1983; Moser 1991; Vinje *et al.* 1993; Bai *et al.* 2007; Červenỳ *et al.* 2007, 2012; Iversen & Tygel 2008) and the finite-difference (FD) method (Vidale 1988; Cao & Greenhalgh 1994; Sethian 1996; Sethian & Popovici 1999; Rawlinson & Sambridge 2004a,b; Noble *et al.* 2014). The ray-tracing method computes the traveltimes by integration along rays in which the initial condition must be specified. The main advantages include easy implementation and high efficiency. However, it gives a non-uniform distribution of traveltimes, and the presence of shadow zones can lead to problems. Moreover, due to the different directions of the group velocity (ray direction) and the phase velocity (wave front normal direction) vectors , solving the ray-tracing system becomes complicated in the anisotropic media. The FD method has been recognized as an efficient and accurate computational scheme for calculating the traveltimes. In the framework of the FD method, two approaches, the fast marching method (Sethian 1996; Sethian & Popovici 1999; Alkhalifah & Fomel 2001; Huang *et al.* 2016b; Huang & Sun 2018) and the fast sweeping method (Zhao 2005), have been widely used for calculating the traveltimes. In recent years, efforts have been made to solve the anisotropic eikonal equations (Luo & Qian 2012; Waheed *et al.* 2015a,b; Bouteiller *et al.* 2017; Han *et al.* 2017; Waheed & Alkhalifah 2017). In addition, some interesting results for moveout approximations have been obtained based on the weak-anisotropy (WA)

parameters (Farra & Pšenčík 2017; Pšenčík & Farra 2017). However, it is challenging to use the FD method to solve the eikonal equation for the anisotropic media because of the additional anisotropic parameters involved. This is especially true because solving the quartic equation and finding the roots of a quartic equation at each computational step are difficult (Alkhalifah 2011a; Stovas & Alkhalifah 2012).

Perturbation theory has been widely used to develop traveltime approximations for calculating the traveltimes in anisotropic media. This approach was proposed by Alkhalifah (2011a,b) for deriving traveltime approximations and scanning anisotropic parameters in transversely isotropic media with a vertical symmetry axis (VTI) and transversely isotropic media with a tilted symmetry axis (TTI) media. Since then, many researchers have applied the perturbation theory and have made significant progress in developing the traveltime approximations. For instance, Stovas & Alkhalifah (2012) derive the traveltime approximations in TTI media by expanding the TTI eikonal equation in a power series in terms of the anellipticity parameter. Subsequent generalizations of the perturbation theory to a transversely isotropic medium can be found in Waheed *et al.* (2013), Alkhalifah (2013) and Masmoudi & Alkhalifah (2016). Xu *et al.* (2017) have applied perturbation theory to moveout approximations in an anisotropic medium. Later, this approach has been extended to an orthorhombic medium (Stovas *et al.* 2016) and attenuating VTI medium (Hao & Alkhalifah 2017).

Recently, we have extended the perturbation theory to the problem of complex traveltime computation. We have applied it to the complex eikonal equations in orthorhombic and VTI media and derived a system of linear equations for the complex traveltime computation. Based on the derived system, we have developed analytic solutions in an orthorhombic medium (Huang & Greenhalgh 2018) and numerical solutions in a VTI medium (Huang *et al.* 2018). The perturbation approach to the complex eikonal equation differs from the real eikonal equation in the following respects. First, we expand the real and imaginary parts of the complex traveltime in terms of the background traveltime and the coefficients separately and transform the problem of the highly nonlinear eikonal equations into one of solving a relatively simple eikonal equation for the background medium and a system of linear partial differential equations. Second, we use a perturbation scheme to solve the background complex eikonal equation for the background traveltimes. In this case, we successfully employed the perturbation theory to solve the complex eikonal equations in anisotropic media.

In reviewing all of the above perturbation theories, we find that most of the traveltime approximations make use of a power-series expansion in terms of the anisotropic parameters and make the assumption of small anisotropic parameters. This means that the degree of anisotropy does not exceed a small perturbation from the elliptically anisotropic background medium. A major limitation of the perturbation analysis technique is that it breaks down in regions with strong anisotropy.

The purpose of this paper is to establish the fundamental theory of the linear partial differential equations for solving the VTI and TTI eikonal equations and to develop traveltime approximations for strongly anisotropic media. To this end, we employ the homotopy analysis method (HAM), an analytic approximation method for highly nonlinear problems, to the nonlinear eikonal equations. The HAM was proposed by Liao (1992c, 1999, 2003a, 2012) for solving nonlinear problems encountered in mathematical physics. Different from the conventional perturbation theory, the HAM does not depend on any physical parameters and can guarantee the convergence of the series solution. This implies that the HAM can be used for arbitrarily high nonlinear problem. From the late 1990s to 2010s, due to the advantages of the HAM over perturbation theory, it has been widely used in the mathematical and physical sciences. Much work has been done on the HAM for nonlinear problems in developing analytic series solutions, for example, nonlinear oscillations (Liao 1992b, 2003b, 2004; Liao & Chwang 1998), boundary layer flows (Liao 1999, 2002), heat transfer (Liao 2003b; Wang *et al.* 2003), nonlinear water waves (Liao 1992a; Liao *et al.* 2016) and nonlinear gravity waves (Liao 2011). In this work, by applying the HAM to anisotropic eikonal equations, we extend the HAM to geophysical problems for anisotropic media.

In the following, we first review the theory of the HAM. After deriving linear partial differential equations in VTI and TTI media, we provide the theoretical background of the differences between the HAM and the perturbation theory and the nature of the derived linear equations. Then, we develop the analytic solutions of the VTI and TTI eikonal equations for traveltime approximations. Finally, we present numerical tests of the contours of the traveltimes and the relative errors which are aimed at quantifying the differences of the results from the HAM and the perturbation theory method and comparing the performance in strongly anisotropic media.

HOMOTOPY ANALYSIS METHOD

The HAM (Liao 2004) is an analytic approximation technique for generating series solutions to highly nonlinear problems. In this method, an embedding parameter q and a convergence control parameter h are chosen to transform the nonlinear equation into a sequence of linear equations. In this section, we review the mathematical formulations of the HAM and discuss the applicability of this method to solving nonlinear equations.

Consider a general nonlinear equation

$$\mathcal{N}[\tau(x,z)] = 0, \tag{1}$$

where $\mathcal{N}$ is a nonlinear operator, x and z are the independent variable parameters, and $\tau(x,z)$ is the exact solution of the nonlinear equation. For solving the above nonlinear equation, Liao (1992a,1992b) developed the zero-order deformation equation

$$(1-q)\,\mathcal{L}\left[t_q(x,z) - \tau_0(x,z)\right] = q\,h\mathcal{H}(x,z)\cdot\mathcal{N}\left[\tau_q(x,z)\right], \tag{2}$$

where $\mathcal{L}$ is an arbitrary linear operator, $\mathcal{H}(x, z)$ is an auxiliary function and $\tau_0(x, z)$ is the initial approximation. Eq. (2) shows that (1) the nonlinear problem is transformed into a linear problem; (2) the linear operator $\mathcal{L}$ plays a crucial role in the transformation; (3) there is a continuous mapping from $\tau(x, z, q)$ to $t(x, z, q)$.

It can be seen that when $q = 0$, eq. (2) becomes

$$\mathcal{L}\left[t_q(x, z) - \tau_0(x, z)\right] = 0, \tag{3}$$

and when $q = 1$, eq. (2) becomes

$$h\mathcal{H}(x, z) \cdot \mathcal{N}\left[\tau_q(x, z)\right] = 0. \tag{4}$$

From eqs (3) and (4), we have

$$t(x, z, 0) = \tau_0(x, z), \tag{5}$$

and

$$t(x, z, 1) = \tau(x, z). \tag{6}$$

Eqs (5) and (6) show that while the embedding parameter q changes from 0 to 1, the solution of the nonlinear eq. (1) varies from the initial approximation to the exact solution of the equation.

By means of Taylor's theorem, the solution of eq. (2) can be expressed as a power series in q to yield the series expansion solution

$$t_q(x, z) = \tau_0(x, z) + \sum_{m=1}^{\infty} \tau_m(x, z) q^m. \tag{7}$$

If now we assume that we can choose the embedding parameter, auxiliary parameter and the auxiliary linear operator to make the series converge at $q = 1$, then we can determine the coefficients by substituting it into eq. (2). Then returning to the situation in which $q = 1$ and from a combination of eqs (6) and (8), we have

$$\tau_q(x, z) = \tau_0(x, z) + \sum_{m=1}^{\infty} \tau_m(x, z). \tag{8}$$

The above solution refers to a situation in which only the coefficients $\tau_m(x, z)$ vary. The solution therefore depends on the initial approximation $\tau_0(x, z)$ and the coefficients $\tau_m(x, z)$. This differs from the perturbation theory in which the solution is a function of the coefficients and small parameters.

The HAM explains how the analytic solutions of the nonlinear equation can be obtained by transforming the nonlinear equation into a linear equation system. From eq. (2), we can observe that with suitable embedding parameter, auxiliary parameter and the auxiliary linear operator, the transformation relationship is always accepted. By analogy with the homotopy analysis process, the first guess approximation is chosen initially for satisfying eq. (3), then the approximation changes until it satisfies eq. (4). This means that the assumed series expansion solution (7) changes from the initial solution to the exact solution. With the embedding parameter q getting larger and larger, the series expansion solution (7) approaches the exact solution smoothly, meaning that, at $q = 1$, the exact solution can be obtained. The homotopy analysis process can be divided into the following steps: (1) choosing the linear operator $\mathcal{L}$; (2) construction of the zero-order deformation equation; (3) determination of the coefficients of the series expansion; (4) obtaining the exact solution by setting $q = 1$.

THEORY FOR TRAVELTIME CALCULATION IN ANISOTROPIC MEDIA USING HAM

In this section, we derive the linearized partial differential equation system for the traveltime solutions of the VTI and TTI eikonal equations by using the HAM. For the VTI eikonal equation, we assume to have the known initial traveltime solution, but just for an elliptically anisotropic medium, which we denote as the background traveltime solution. We start with Alkhalifah's acoustic eikonal equation for a VTI medium involving the anisotropic parameter η. Following recent work (Huang & Greenhalgh 2018; Huang *et al.* 2018), we choose the linear operator form as an elliptical anisotropic eikonal equation. Then, we propose the solution as a series expansion containing the embedding parameter q. For the TTI eikonal equation, the initial solution and linear operator are chosen in a similar way to the VTI eikonal equation. However, for the series expansion, we only keep two terms because if we keep high-order terms, the solution of the TTI eikonal equation is complicated.

Retrieved VTI eikonal equation

Following Alkhalifah (2000), the eikonal equation for VTI media can be written as

$$v^2(1 + 2\eta)\left(\frac{\partial \tau}{\partial x}\right)^2 + v_v^2\left(\frac{\partial \tau}{\partial z}\right)^2\left(1 - 2\eta v_v^2\left(\frac{\partial \tau}{\partial x}\right)^2\right) = 1. \tag{9}$$

Here, $\tau(x, z)$ is the traveltime at the position in the coordinates (x, z) , v is the P-wave normal-moveout (NMO) velocity ($v = v_v\sqrt{1+2\delta}$), v_v is the vertical P-wave velocity and η is the anellipticity parameter. According to eqs (2) and () and by choosing the linear operator as

$$\mathcal{L} = v^2 \frac{\partial \tau_0}{\partial x}\frac{\partial \tau}{\partial x} + v_v^2 \frac{\partial \tau_0}{\partial z}\frac{\partial \tau}{\partial z}, \tag{10}$$

and the nonlinear operator as

$$\mathcal{N} = v^2(1+2\eta)\left(\frac{\partial \tau}{\partial x}\right)^2 + v_v^2\left(\frac{\partial \tau}{\partial z}\right)^2\left(1 - 2\eta v^2\left(\frac{\partial \tau}{\partial x}\right)^2\right) - 1, \tag{11}$$

we obtain the following zero-order deformation equation for the eikonal equation in VTI media

$$(1-q)\left(v^2\frac{\partial \tau_0}{\partial x}\frac{\partial \tau}{\partial x} + v_v^2\frac{\partial \tau_0}{\partial z}\frac{\partial \tau}{\partial z} - \left(v^2\left(\frac{\partial \tau_0}{\partial x}\right)^2 + v_v^2\left(\frac{\partial \tau_0}{\partial z}\right)^2\right)\right) + q\left(v^2(1+2\eta)\left(\frac{\partial \tau}{\partial x}\right)^2 + v_v^2\left(\frac{\partial \tau}{\partial z}\right)^2\left(1 - 2\eta v^2\left(\frac{\partial \tau}{\partial x}\right)^2\right) - 1\right) = 0, \tag{12}$$

where τ_0 is the traveltime solution (initial approximation) for the elliptical anisotropic eikonal equation. To obtain the linear equation system, we assume

$$\tau = \tau_0 + \tau_1 q + \tau_2 q^2 + \tau_3 q^3, \tag{13}$$

where τ_1, τ_2 and τ_3 are the first-order, second-order and third-order coefficients, respectively. Then substituting eq. (13) into eq. (12), we obtain the linear partial differential equation for the first-order coefficient τ_1:

$$\left(\frac{\partial \tau_0}{\partial x}\right)\left(\frac{\partial \tau_1}{\partial x}\right)v^2 + \left(\frac{\partial \tau_0}{\partial z}\right)\left(\frac{\partial \tau_1}{\partial z}\right)v_v^2 = 2\eta\left(\frac{\partial \tau_0}{\partial x}\right)^2\left(\frac{\partial \tau_0}{\partial z}\right)^2 v_v^2 v^2 - (2\eta+1)\left(\frac{\partial \tau_0}{\partial x}\right)^2 v^2 - \left(\frac{\partial \tau_0}{\partial z}\right)^2 v_v^2 + 1, \tag{14}$$

the linear partial differential equation for the second-order coefficient τ_2:

$$\begin{aligned}\left(\frac{\partial \tau_0}{\partial x}\right)\left(\frac{\partial \tau_2}{\partial x}\right)v^2 + \left(\frac{\partial \tau_0}{\partial z}\right)\left(\frac{\partial \tau_2}{\partial z}\right)v_v^2 &= 4\eta\left(\frac{\partial \tau_0}{\partial x}\right)^2\left(\frac{\partial \tau_0}{\partial z}\right)\left(\frac{\partial \tau_1}{\partial z}\right)v_v^2 v^2 + 4\eta\left(\frac{\partial \tau_0}{\partial x}\right)\left(\frac{\partial \tau_0}{\partial z}\right)^2\left(\frac{\partial \tau_1}{\partial x}\right)v_v^2 v^2 \\ &\quad - 2(2\eta+1)\left(\frac{\partial \tau_0}{\partial x}\right)\left(\frac{\partial \tau_1}{\partial x}\right)v^2 - \left(\frac{\partial \tau_0}{\partial x}\right)\left(\frac{\partial \tau_1}{\partial z}\right)v^2 - \left(\frac{\partial \tau_0}{\partial z}\right)\left(\frac{\partial \tau_1}{\partial z}\right)v_v^2\end{aligned} \tag{15}$$

and the linear partial differential equation for the third-order coefficient τ_3:

$$\begin{aligned}\left(\frac{\partial \tau_0}{\partial x}\right)\left(\frac{\partial \tau_3}{\partial x}\right)v^2 + \left(\frac{\partial \tau_0}{\partial z}\right)\left(\frac{\partial \tau_3}{\partial x}\right)v_v^2 &= 4\eta\left(\frac{\partial \tau_0}{\partial x}\right)^2\left(\frac{\partial \tau_0}{\partial z}\right)\left(\frac{\partial \tau_2}{\partial z}\right)v_v^2 v^2 + 2\eta\left(\frac{\partial \tau_0}{\partial x}\right)^2\left(\frac{\partial \tau_1}{\partial z}\right)^2 v_v^2 v^2 + 4\eta\left(\frac{\partial \tau_0}{\partial x}\right)\left(\frac{\partial \tau_0}{\partial z}\right)^2\left(\frac{\partial \tau_2}{\partial x}\right)v_v^2 v^2 \\ &\quad + 8\eta\left(\frac{\partial \tau_0}{\partial x}\right)\left(\frac{\partial \tau_0}{\partial z}\right)\left(\frac{\partial \tau_1}{\partial x}\right)\left(\frac{\partial \tau_1}{\partial z}\right)v_v^2 v^2 - 2(2\eta+1)\left(\frac{\partial \tau_0}{\partial x}\right)\left(\frac{\partial \tau_2}{\partial x}\right)v^2 + \left(\frac{\partial \tau_0}{\partial x}\right)\left(\frac{\partial \tau_2}{\partial x}\right)v^2 \\ &\quad + 2\eta\left(\frac{\partial \tau_0}{\partial z}\right)^2\left(\frac{\partial \tau_1}{\partial x}\right)^2 v_v^2 v^2 - \left(\frac{\partial \tau_0}{\partial z}\right)\left(\frac{\partial \tau_2}{\partial z}\right)v_v^2 - (2\eta+1)\left(\frac{\partial \tau_1}{\partial x}\right)^2 v^2 - \left(\frac{\partial \tau_1}{\partial z}\right)^2 v_v^2.\end{aligned} \tag{16}$$

The linearized partial differential equations, derived in this section, may be used directly for obtaining the coefficients τ_1, τ_2 and τ_3, once the initial traveltime solution τ_0 has been calculated. For each linear equation, we can solve the equation for the corresponding coefficient in terms of the anisotropic parameter. Thus, instead of solving the eikonal equation in VTI media directly, we can obtain the solutions by solving the above linearized partial differential equations.

Retrieved TTI eikonal equation

The eikonal equation for TTI media is given by (Alkhalifah 2000)

$$v^2(1+2\eta)\left(\frac{\partial \tau}{\partial x}\cos\theta + \frac{\partial \tau}{\partial z}\sin\theta\right)^2 + v_t^2\left(\frac{\partial \tau}{\partial z}\cos\theta - \frac{\partial \tau}{\partial x}\sin\theta\right)^2\left(1 - 2\eta v^2\left(\frac{\partial \tau}{\partial x}\cos\theta + \frac{\partial \tau}{\partial z}\sin\theta\right)^2\right) = 1, \tag{17}$$

where θ is the angle of the symmetry axis measured from the vertical direction and v_t is the tilted velocity. According to eqs (2) and (7) and by choosing the linear operator as

$$\mathcal{L} = v^2\frac{\partial \tau_0}{\partial x}\frac{\partial \tau}{\partial x} + v_t^2\frac{\partial \tau_0}{\partial z}\frac{\partial \tau}{\partial z} \tag{18}$$

and the nonlinear operator as

$$\mathcal{N} = v^2(1+2\eta)\left(\frac{\partial \tau}{\partial x}\cos\theta + \frac{\partial \tau}{\partial z}\sin\theta\right)^2 + v_t^2\left(\frac{\partial \tau}{\partial z}\cos\theta - \frac{\partial \tau}{\partial x}\sin\theta\right)^2\left(1 - 2\eta v^2\left(\frac{\partial \tau}{\partial x}\cos\theta + \frac{\partial \tau}{\partial z}\sin\theta\right)^2\right) - 1, \tag{19}$$

we obtain the following zero-order deformation equation for the eikonal equation in TTI media:

$$(1-q)\left(v^2\frac{\partial\tau_0}{\partial x}\frac{\partial\tau}{\partial x}+v_t^2\frac{\partial\tau_0}{\partial z}\frac{\partial\tau}{\partial z}-\left(v^2\left(\frac{\partial\tau_0}{\partial x}\right)^2+v_t^2\left(\frac{\partial\tau_0}{\partial z}\right)^2\right)\right)$$
$$+q\left(v^2(1+2\eta)\left(\frac{\partial\tau}{\partial x}\cos\theta+\frac{\partial\tau}{\partial z}\sin\theta\right)^2+v_t^2\left(\frac{\partial\tau}{\partial z}\cos\theta-\frac{\partial\tau}{\partial x}\sin\theta\right)^2\left(1-2\eta v^2\left(\frac{\partial\tau}{\partial x}\cos\theta+\frac{\partial\tau}{\partial z}\sin\theta\right)^2\right)-1\right)=0, \tag{20}$$

where τ_0 is the traveltime solution (initial approximation) for the elliptical anisotropic eikonal equation.

In a similar manner, by assuming

$$\tau=\tau_0+\tau_1 q+\tau_2 q^2, \tag{21}$$

we obtain the following linear partial differential equations for the first-order and second-order coefficients τ_1 and τ_2, respectively:

$$\begin{aligned}-\frac{\partial\tau_0}{\partial x}\frac{\partial\tau_1}{\partial x}v^2-\frac{\partial\tau_0}{\partial z}\frac{\partial\tau_1}{\partial z}v_t^2=&-2\eta\left(\frac{\partial\tau_0}{\partial x}\right)^4v^2v_v^2\sin^2\theta\cos^2\theta+4\eta\left(\frac{\partial\tau_0}{\partial x}\right)^3\frac{\partial\tau_0}{\partial z}v^2v_t^2\sin\theta\cos^3\theta-4\eta\left(\frac{\partial\tau_0}{\partial x}\right)\frac{\partial\tau_0}{\partial z}v^2v_t^2\sin^3\theta\cos\theta\\&-2\eta\left(\frac{\partial\tau_0}{\partial x}\right)^2\left(\frac{\partial\tau_0}{\partial z}\right)^2v^2v_t^2\sin^4\theta-2\eta\left(\frac{\partial\tau_0}{\partial x}\right)^2\left(\frac{\partial\tau_0}{\partial z}\right)^2v^2v_t^2\cos^4\theta\\&+8\eta\left(\frac{\partial\tau_0}{\partial x}\right)^2\left(\frac{\partial\tau_0}{\partial z}\right)^2v^2v_t^2\sin^2\theta\cos^2\theta\\&+(2\eta+1)\left(\frac{\partial\tau_0}{\partial x}\right)^2v^2\cos^2\theta+\left(\frac{\partial\tau_0}{\partial x}\right)^2v_t^2\sin^2\theta-4\eta\frac{\partial\tau_0}{\partial x}\left(\frac{\partial\tau_0}{\partial z}\right)^3v^2v_t^2\sin\theta\cos^3\theta\\&+4\eta\frac{\partial\tau_0}{\partial x}\left(\frac{\partial\tau_0}{\partial z}\right)^3v^2v_t^2\sin^3\theta\cos\theta\\&+2(2\eta+1)\left(\frac{\partial\tau_0}{\partial x}\right)^2v^2\sin\theta\cos\theta-2\frac{\partial\tau_0}{\partial x}\frac{\partial\tau_0}{\partial z}v_t^2\sin\theta\cos\theta-2\eta\left(\frac{\partial\tau_0}{\partial z}\right)^4v^2v_t^2\sin^2\theta\cos^2\theta\\&+(2\eta+1)\left(\frac{\partial\tau_0}{\partial z}\right)^2v^2\sin^2\theta+\left(\frac{\partial\tau_0}{\partial z}\right)^2v_t^2\cos^2\theta-1\end{aligned} \tag{22}$$

and

$$\begin{aligned}-\frac{\partial\tau_0}{\partial x}\frac{\partial\tau_2}{\partial x}v^2-\frac{\partial\tau_0}{\partial z}\frac{\partial\tau_2}{\partial z}v_t^2=&-8\eta\left(\frac{\partial\tau_0}{\partial x}\right)^3\frac{\partial\tau_1}{\partial x}v^2v_t^2\sin^2\theta\cos^2\theta+4\eta\left(\frac{\partial\tau_0}{\partial x}\right)^3\frac{\partial\tau_1}{\partial z}v^2v_t^2\sin\theta\cos^3-4\eta\left(\frac{\partial\tau_0}{\partial x}\right)^3\frac{\partial\tau_1}{\partial z}v^2v_t^2\sin^3\theta\cos\theta\\&+12\eta\left(\frac{\partial\tau_0}{\partial x}\right)^2\frac{\partial\tau_0}{\partial z}\frac{\partial\tau_1}{\partial x}v^2v_t^2\sin\theta\cos^3\theta-12\eta\left(\frac{\partial\tau_0}{\partial x}\right)^2\frac{\partial\tau_0}{\partial z}\left(\frac{\partial\tau_1}{\partial x}\right)v^2v_t^2\sin^3\theta\cos\theta\\&-4\eta\left(\frac{\partial\tau_0}{\partial x}\right)^2\frac{\partial\tau_0}{\partial z}\frac{\partial\tau_1}{\partial z}v^2v_t^2\sin^4\theta\\&-4\eta\left(\frac{\partial\tau_0}{\partial x}\right)^2\frac{\partial\tau_0}{\partial z}\frac{\partial\tau_1}{\partial z}v^2v_t^2\cos^4\theta+16\eta\left(\frac{\partial\tau_0}{\partial x}\right)^2\frac{\partial\tau_0}{\partial z}\frac{\partial\tau_1}{\partial z}v^2v_t^2\sin^2\theta\cos^2\theta\\&-4\eta\frac{\partial\tau_0}{\partial x}\left(\frac{\partial\tau_0}{\partial z}\right)^2\frac{\partial\tau_1}{\partial x}v^2v_t^2\sin^4\theta\\&-4\eta\frac{\partial\tau_0}{\partial x}\left(\frac{\partial\tau_0}{\partial z}\right)^2\frac{\partial\tau_1}{\partial x}v^2v_t^2\cos^4\theta+16\eta\left(\frac{\partial\tau_0}{\partial x}\right)\left(\frac{\partial\tau_0}{\partial z}\right)^2\frac{\partial\tau_1}{\partial x}v^2v_t^2\sin^2\theta\cos^2\theta\\&-12\eta\frac{\partial\tau_0}{\partial x}\left(\frac{\partial\tau_0}{\partial z}\right)^2\frac{\partial\tau_1}{\partial z}v^2v_t^2\sin\theta\cos^3\theta\\&+12\eta\frac{\partial\tau_0}{\partial x}\left(\frac{\partial\tau_0}{\partial z}\right)^2\frac{\partial\tau_1}{\partial z}v^2v_t^2\sin^3\theta\cos\theta+2\frac{\partial\tau_0}{\partial x}\frac{\partial\tau_1}{\partial x}v_t^2\sin^2\theta+2(2\eta+1)\frac{\partial\tau_0}{\partial x}\frac{\partial\tau_1}{\partial z}v^2\sin\theta\cos\theta\\&-2\frac{\partial\tau_0}{\partial x}\frac{\partial\tau_1}{\partial z}v_t^2\sin\theta\cos\theta\\&-4\eta\left(\frac{\partial\tau_0}{\partial z}\right)^3\frac{\partial\tau_1}{\partial x}v^2v_t^2\sin\theta\cos^3\theta+4\eta\left(\frac{\partial\tau_0}{\partial z}\right)^3\frac{\partial\tau_1}{\partial x}v^2v_t^2\sin^3\theta\cos\theta-8\eta\left(\frac{\partial\tau_0}{\partial z}\right)^3\frac{\partial\tau_1}{\partial z}v^2v_t^2\sin^2\theta\cos^2\theta\\&-2\frac{\partial\tau_0}{\partial z}\frac{\partial\tau_1}{\partial x}v_t^2\sin\theta\cos\theta+2(2\eta+1)\frac{\partial\tau_0}{\partial z}\frac{\partial\tau_0}{\partial z}v^2\sin^2\theta-\frac{\partial\tau_0}{\partial z}\frac{\partial\tau_1}{\partial z}v_t^2+2\frac{\partial\tau_0}{\partial z}\frac{\partial\tau_1}{\partial z}v_t^2\cos^2\theta.\end{aligned} \tag{23}$$

Differences between HAM and perturbation theory

There is another approach to solving the eikonal equation in an anisotropic medium without having to find the root of a quartic equation as in the FD method. The perturbation method using a Taylor series expansion is by far the most widespread approach developed by Alkhalifah (2011a,b) and Stovas & Alkhalifah (2012). Such an approach has been adopted by many researchers (Stovas & Alkhalifah 2012; Alkhalifah 2013; Waheed *et al.* 2013; Masmoudi & Alkhalifah 2016; Stovas *et al.* 2016) for solving anisotropic eikonal equations. Recently, we applied this method to the complex eikonal equation for the seismic complex traveltime (Huang & Greenhalgh 2018; Huang *et al.* 2018). The perturbation method enables transforming the nonlinear problem into linear problems that can be used to derive analytic solutions of the anisotropic eikonal equation or solved by the FD method for numerical solutions. This reduces to a simple iteration scheme for the linearized partial difference equation system. Now we discuss the differences between the HAM and perturbation method and show why the HAM can account for a strongly anisotropic medium.

For VTI media, the perturbation expansion based on the Taylor series expansion is given by (Alkhalifah 2011a)

$$\tau = \tau_0 + \tau_1\eta + \tau_2\eta^2, \tag{24}$$

where τ_1 and τ_2 are the first-order and second-order coefficients of the Taylor series expansion, respectively.

For TTI media, the perturbation expansion based on the Taylor series expansion is given by (Alkhalifah 2011b)

$$\tau = \tau_0 + \tau_\eta\eta + \tau_\theta \sin\theta + \tau_{\eta_2}\eta^2 + \tau_{\eta\theta}\eta\sin\theta + \tau_{\theta_2}\sin^2\theta, \tag{25}$$

where τ_η, τ_θ, τ_{η_2}, $\tau_{\eta\theta}$ and τ_{θ_2} are the coefficients. Another approach for the TTI eikonal equation given by Stovas & Alkhalifah (2012) is

$$\tau = \tau_0 + \tau_{\eta 1}\eta + \tau_{\eta 2}\eta^2, \tag{26}$$

where $\tau_{\eta 1}$ and $\tau_{\eta 2}$ are the first-order and second-order coefficients of the Taylor series expansion, respectively.

The most obvious difference between the HAM and the perturbation method is their different expansion parameters in the expansion series. In the case of the perturbation method shown as eqs (24)–(26), the traveltime is expressed as a Taylor series expansion with respect to the small anisotropic parameters η and θ. In the perturbation expansion, there is an assumption of small perturbation, meaning that the anisotropic parameter is small. In the case of the HAM, the series expansion depends on the embedding parameter q. Contrary to the perturbation method, which is characterized by a Taylor series expansion that becomes the solution after obtaining the coefficients, the series expansion using the HAM approaches the exact solution with an increasing embedding parameter q, arriving at the exact analytic solution where $q = 1$.

Comparison of eqs (13) and (21) with eqs (24)–(26) implies two options for solving the anisotropic eikonal equations. One is to take the traveltime with respect to the anisotropic parameters; the other is to use the series expansion with respect to the embedding parameter q. A major feature of the former approach is the handling of lateral variation in η and θ. The perturbation method is only good for estimating constant η in a velocity analysis framework. However, the two methods have different capabilities for computing the traveltime in anisotropic media with lateral variation because of the different forms of the series expansions. In this case, since there is not the assumption of small perturbation in the HAM, this method can be used for a strongly anisotropic medium.

TRAVELTIME APPROXIMATION

One primary aim of this paper is to develop an analytic solution of the eikonal equation in homogeneous VTI and TTI media. To this end, we start with the initial traveltime solution satisfying the elliptical anisotropic eikonal equation and apply this solution to the linearized partial differential equations derived in the last section to obtain the coefficients of the series expansions (13) and (21). Then, we obtain the analytic solution of the eikonal equations in the anisotropic medium.

Analytical formulae for traveltime in VTI media

The analytic formula for the elliptical anisotropic eikonal equation is given by (Alkhalifah 2011a)

$$\tau_0 = \sqrt{\frac{x^2}{v^2} + \frac{z^2}{v_v^2}}. \tag{27}$$

Substituting eq. (27) into eq. (14), we obtain

$$\tau_1 = -\frac{2\eta v_v^4 x^4 \sqrt{\frac{x^2}{v^2} + \frac{z^2}{v_v^2}}}{\left(v^2 z^2 + v_v^2 x^2\right)^2}. \tag{28}$$

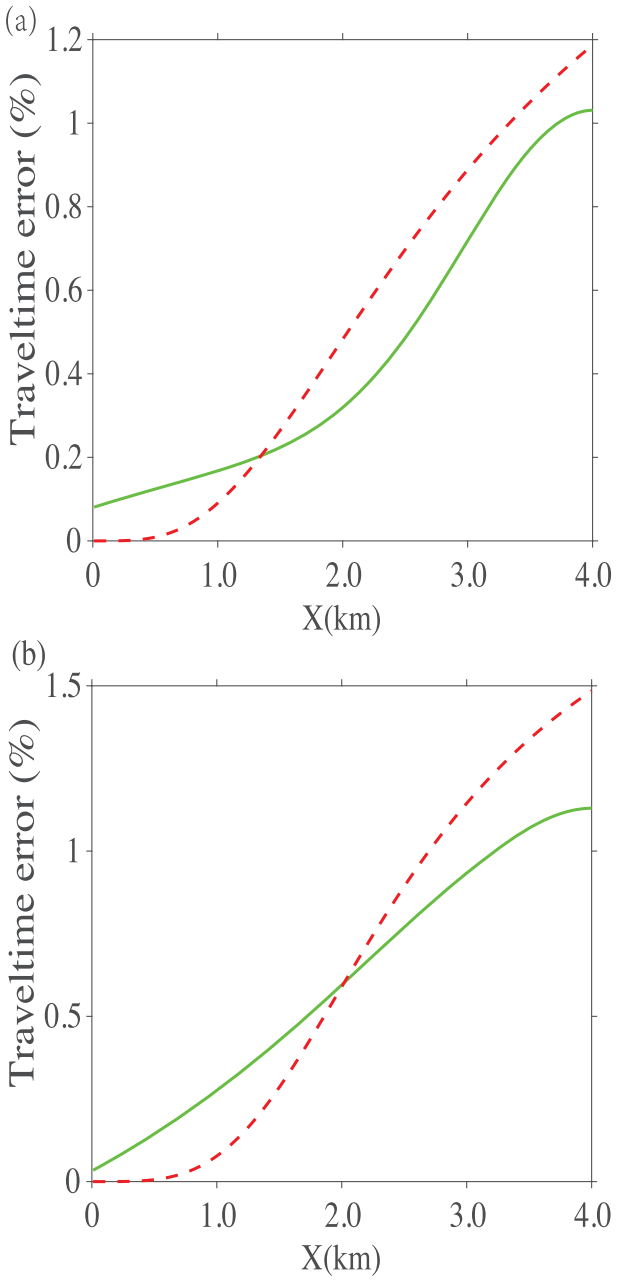

Figure 1. Comparison of the percentage traveltime error as a function of offset at the depth of 2 km using the perturbation method (dash red line) and the homotopy analysis method (solid green line) in VTI media with $C_{11} = 6.3$, $C_{13} = 2.25$, $C_{33} = 4.51$, $C_{44} = 1.0$, $C_{66} = 1.5$ ($\eta = 0.28$, $\varepsilon = 0.19$ and $\delta = -0.05$) for panel (a) and $C_{11} = 25.7$, $C_{13} = 15.2$, $C_{33} = 15.4$, $C_{44} = 4.2$, $C_{66} = 9.0$ ($\eta = -0.16$, $\varepsilon = 0.33$ and $\delta = 0.72$) for panel (b).

Also, applying eqs (27) and (28) to eq. (15), we have

$$\tau_2 = \frac{2\eta v_v^4 x^4 \sqrt{\frac{x^2}{v^2} + \frac{z^2}{v_v^2}} \left(v^4 z^4 + 2(14\eta + 1) v^2 v_v^2 x^2 z^2 + (4\eta + 1) v_v^4 x^4\right)}{\left(v^2 z^2 + v_v^2 x^2\right)^4}. \tag{29}$$

Furthermore, inserting eqs (27)–(29) into eq. (16) gives

$$\tau_3 = -\frac{4\eta v_v^4 x^4 \sqrt{\frac{x^2}{v^2} + \frac{z^2}{v_v^2}} \left(v^8 z^8 + 2(29\eta + 2) v^6 v_v^2 x^2 z^6 + 3(\eta(248\eta + 41) + 2) v^4 v_v^4 x^4 z^4 + 2(\eta(36 - 13\eta) + 2) v^2 v_v^6 x^6 z^2 + (2\eta + 1)(5\eta + 1) v_v^8 x^8\right)}{\left(v^2 z^2 + v_v^2 x^2\right)^6}. \tag{30}$$

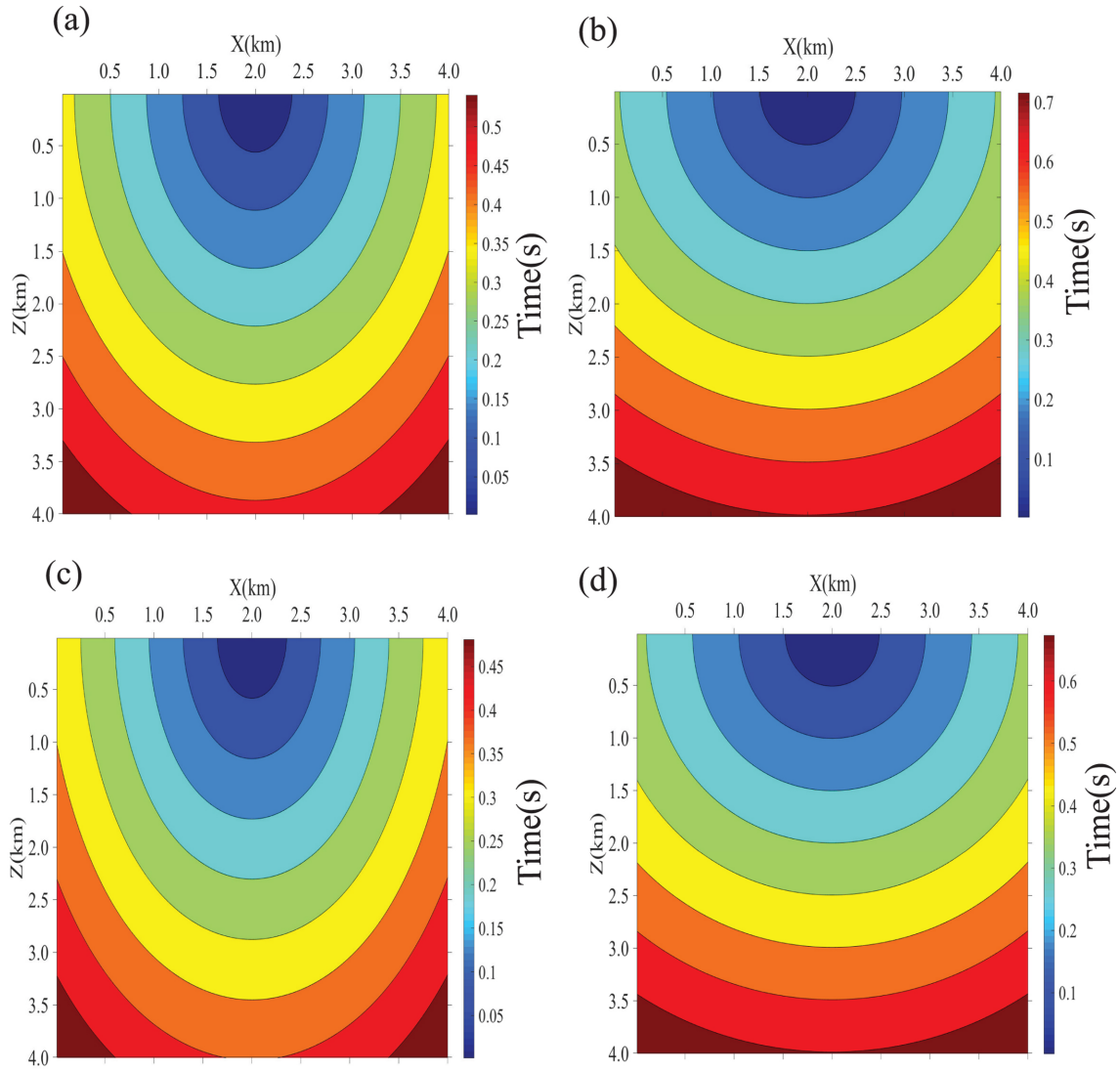

Figure 2. Colour plot of contours of the traveltime in VTI media. (a and c) The homotopy analysis method; (b and d) the perturbation method. The elastic parameters are $C_{11} = 35.7$, $C_{13} = 15.2$, $C_{33} = 15.4$, $C_{44} = 4.2$, $C_{66} = 9.0$ ($\eta = 0.03$, $\varepsilon = 0.66$ and $\delta = 0.58$) for panels (a) and (b), and $C_{11} = 40.7$, $C_{13} = 17.2$, $C_{33} = 15.4$, $C_{44} = 4.2$, $C_{66} = 9.0$ ($\eta = 0.04$, $\varepsilon = 0.82$ and $\delta = 0.81$) for panels (c) and (d).

Analytical formulae for traveltime in TTI media

For the analytic solution of the TTI eikonal equation, we employ the same initial traveltime solution to obtain the corresponding coefficients. The analytic formula for the elliptical anisotropic eikonal equation can be written as

$$\tau_0 = \sqrt{\frac{x^2}{v^2} + \frac{z^2}{v_t^2}}. \tag{31}$$

A derivation for the analytic solutions for the traveltime in homogeneous TTI media based on the initial solution for an elliptical anisotropic background medium is provided in the Appendix.

RESULTS

Comparison of HAM with perturbation method

To validate and test the accuracy of the analytic formulae using the HAM, we first compute the traveltimes in homogeneous VTI media. Here we use the group velocity formulae given by Zhou & Greenhalgh (2004) to construct the wave fronts. The phase velocity is given by

$$c_1 = \sqrt{P \pm \sqrt{P^2 - Q}} \tag{32}$$

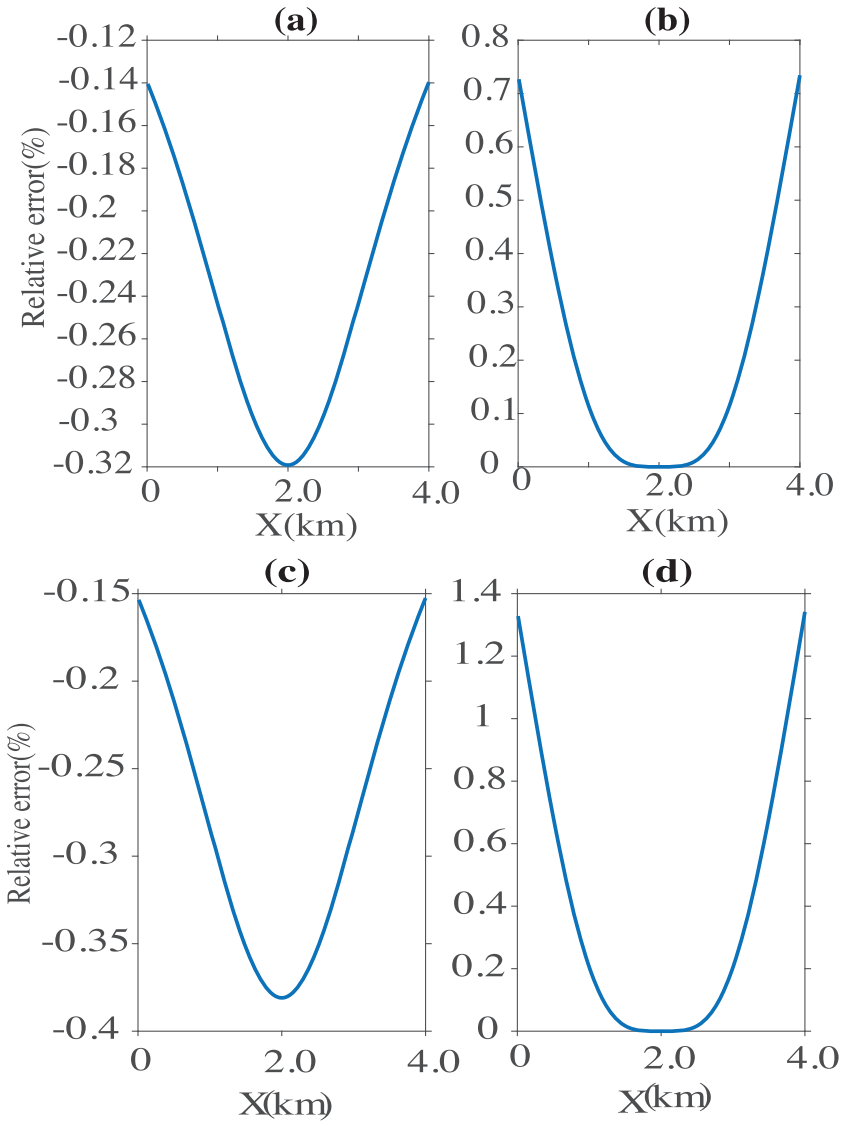

Figure 3. The percentage relative errors of the traveltime at a depth of 2 km for homogeneous VTI media using the homotopy analysis method (panels a and c) and perturbation method (panels b and d).The size of the model is 4 km × 4 km. The source is located at (2 km, 10 m). The elastic parameters are $C_{11} = 35.7$, $C_{13} = 15.2$, $C_{33} = 15.4$, $C_{44} = 4.2$, $C_{66} = 9.0$ ($\eta = -0.03$, $\varepsilon = 0.66$ and $\delta = 0.72$) for panels (a) and (b), and $C_{11} = 40.7$, $C_{13} = 17.2$, $C_{33} = 15.4$, $C_{44} = 4.2$, $C_{66} = 9.0$ ($\eta = -0.04$, $\varepsilon = 0.82$ and $\delta = 0.81$) for panels (c) and (d).

where

$$P = \frac{Q_1 + Q_2}{2},\ Q = Q_1 Q_2 - Q_3 \tag{33}$$

with

$$\begin{cases} Q_1 = C_{44} + (C_{11} - C_{44}) \sin^2 \vartheta \\ Q_2 = C_{33} + (C_{44} - C_{33}) \sin^2 \vartheta \\ Q_3 = 0.25(C_{13} + C_{44})^2 \sin^2 2\vartheta \end{cases}. \tag{34}$$

Then, the group velocity can be written as

$$U_1 = \sqrt{c_1^2 + \left(\frac{\partial c_1}{\partial \vartheta}\right)^2} \tag{35}$$

where

$$\frac{\partial c_1}{\partial \vartheta} = \frac{1}{2c_1}\left[\frac{\partial P}{\partial \vartheta} \pm \frac{1}{\sqrt{P^2 - Q}}\left(P\frac{\partial P}{\partial \vartheta} - 0.5\frac{\partial Q}{\partial \vartheta}\right)\right] \tag{36}$$

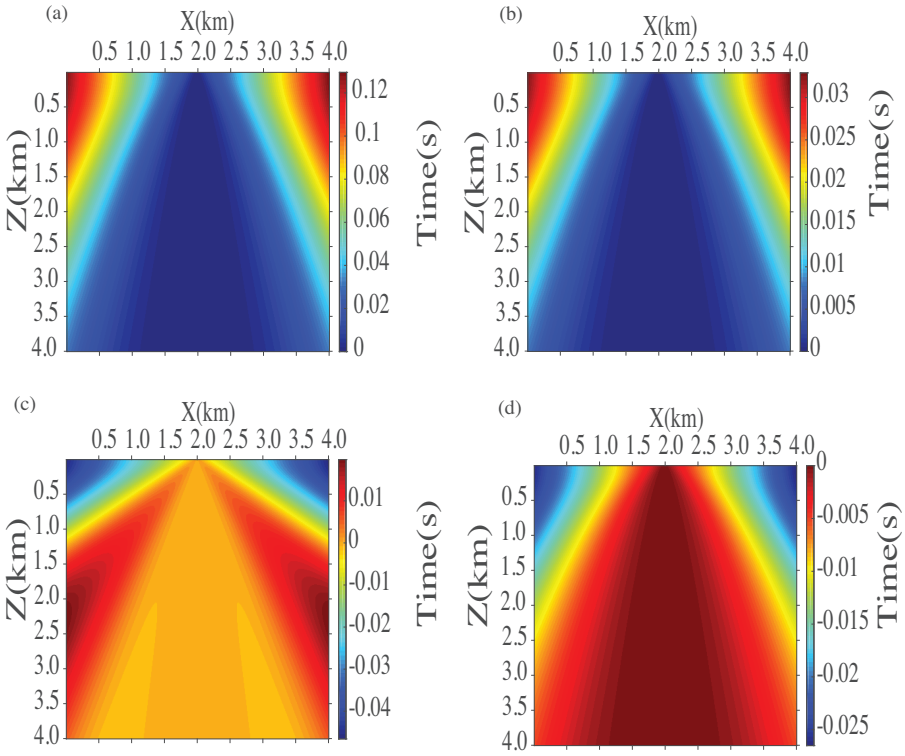

Figure 4. Colour plot of coefficients of the traveltime expansion. Panels (a) and (b) show the first-order expansion coefficient; panels (c) and (d) show the second-order expansion coefficient. The elastic parameters are $C_{11} = 25.7$, $C_{13} = 15.2$, $C_{33} = 15.4$, $C_{44} = 4.2$, $C_{66} = 9.0$ ($\eta = 0.16$, $\varepsilon = 0.33$ and $\delta = 0.81$) for panels (a) and (c), and $C_{11} = 35.7$, $C_{13} = 17.2$, $C_{33} = 15.4$, $C_{44} = 4.2$, $C_{66} = 9.0$ ($\eta = 0.1$, $\varepsilon = 0.66$ and $\delta = 0.92$) for panels (b) and (d).

with

$$\frac{\partial P}{\partial \vartheta} = 0.5\,(C_{11} - C_{33}) \sin 2\vartheta \tag{37}$$

and

$$\frac{\partial Q}{\partial \vartheta} = [Q_1\,(C_{44} - C_{33}) + Q_2\,(C_{11} - C_{44})] \sin 2\vartheta - 0.5\,(C_{13} + C_{44})^2 \sin 4\vartheta\,. \tag{38}$$

We will use the traveltimes constructed using the above formulae as the reference traveltimes and compare the relative error of traveltimes using the HAM and the perturbation method.

Fig. 1 shows the comparison of the traveltime error as a function of offset at the depth of 2 km using the perturbation method (red dash line) and the HAM (green solid line) in VTI media with $C_{11} = 6.3$, $C_{13} = 2.25$, $C_{33} = 4.51$, $C_{44} = 1.0$, $C_{66} = 1.5$ ($\eta = 0.28$, $\varepsilon = 0.19$ and $\delta = -0.05$) for (a) and $C_{11} = 25.7$, $C_{13} = 15.2$, $C_{33} = 15.4$, $C_{44} = 4.2$, $C_{66} = 9.0$ ($\eta = -0.16$, $\varepsilon = 0.33$ and $\delta = 0.72$) for (b). The size of the model is 4 km $\times$ 4 km and the source is located at (10 m, 10 m). In this computation, we use the traveltimes from the exact solution (Zhou & Greenhalgh 2004) in the actual medium as the reference traveltimes. From Fig. 1, we can observe that the relative errors of both methods increase gradually with increasing distance in the x-direction. At around 4 km in the x-direction, the relative error arrives at the maximum value of 1. This can be easily explained. The larger the distance from the source, the larger errors will be. However, when the distance in the x-direction is less than 2 km, the values of the relative error using the HAM are bigger than those from the perturbation method. For a large offset, the results using the formulae from the HAM have a higher accuracy.

Traveltimes in strongly anisotropic media

To examine the capabilities of the analytic formulae developed in this paper and compare the results with the results from the perturbation method, we compute the traveltimes and their relative errors in more strongly anisotropic media. The size of the model is 4 km $\times$ 4 km and the source is located at (2 km, 10m). Fig. 2 shows a colour plot of the contours of the traveltimes. Figs 2(a) and (c) show the results using the HAM and Figs 2(b) and (d) show the results using the perturbation method. The elastic parameters are $C_{11} = 35.7$, $C_{13} = 15.2$, $C_{33} = 15.4$, $C_{44} = 4.2$, $C_{66} = 9.0$ ($\eta = 0.03$, $\varepsilon = 0.66$ and $\delta = 0.58$) for (a) and (b), and $C_{11} = 40.7$, $C_{13} = 17.2$, $C_{33} = 15.4$, $C_{44} = 4.2$, $C_{66} = 9.0$ ($\eta = 0.04$, $\varepsilon = 0.82$ and $\delta = 0.81$) for (c) and (d). From Fig. 2, it can be seen that although all the formulae yield smooth, continuous

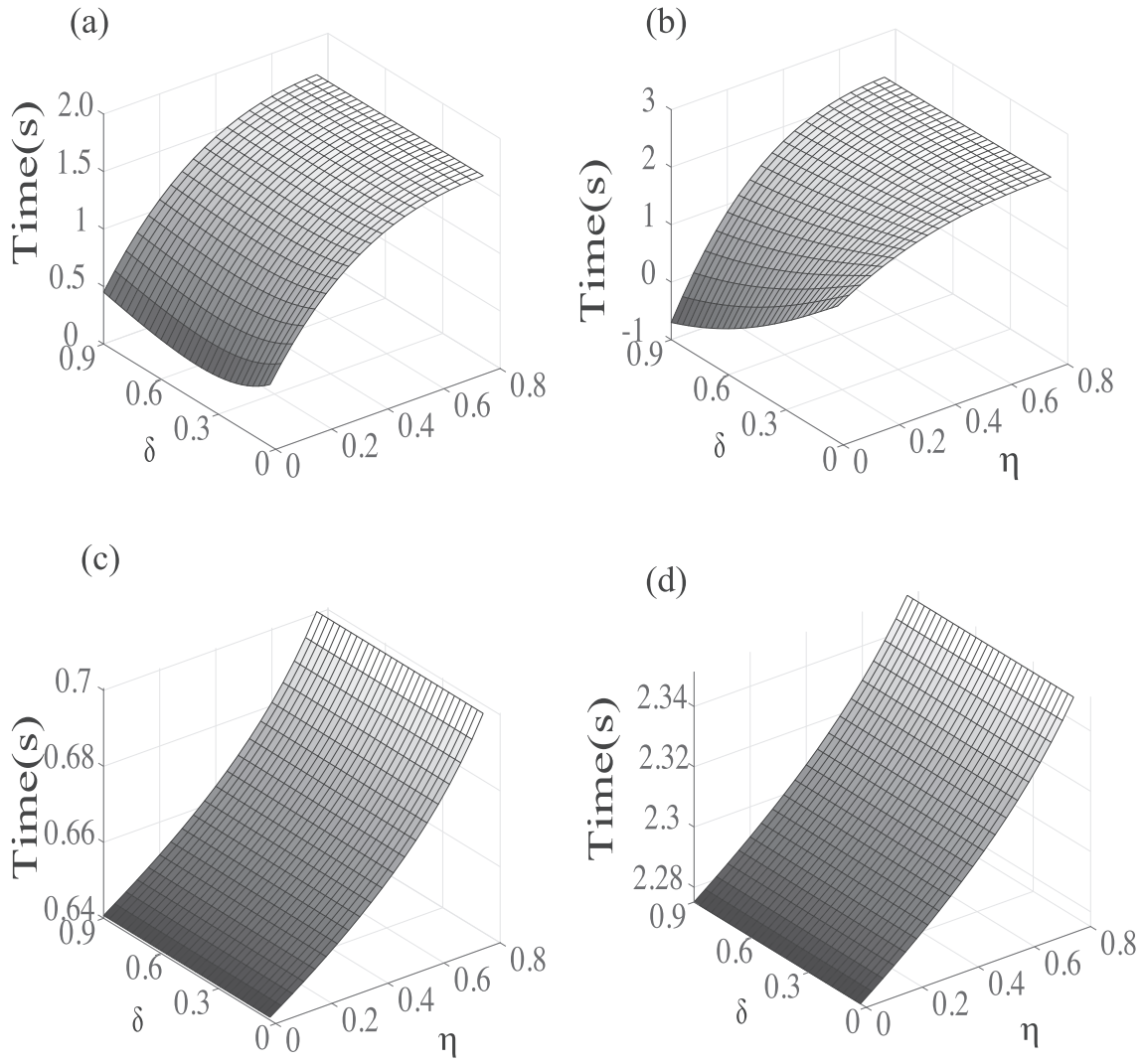

Figure 5. Effects of the anisotropic parameters on the traveltimes. The size of the model is 4 km × 4 km and the source is located at (2 km, 10 m). Panels (a) and (b) show results using the homotopy analysis method at the locations of (1 km, 1 km) and (2.5 km, 4 km); panels (c) and (d) show the results using the perturbation method at the locations of (1 km, 1 km) and (2.5 km, 4 km).

contours of the traveltime, there is some difference in the region far from the source. Comparing Figs 2(a) and (c) with Figs 2(b) and (d), one can recognize the difference between the results from the two methods. Specifically, by applying the chosen embedding parameter q and the HAM, the traveltime formulae can include the anisotropic parameters. By contrast, the analytic formulae with the perturbation method cannot give an accurate result in a strongly anisotropic medium but only give the results with a small perturbation of the anisotropic parameter. The difference in the results is caused mainly by the anisotropic parameters in which the traveltimes have different sensitivity behaviours to the various anisotropic parameters.

Fig. 3 shows the comparison of the relative errors of the traveltimes at a depth of 2 km using the perturbation method (b and d) and HAM (a and c). The experiments show that traveltime formulae with different methods can yield differing accuracy in the traveltime computation. From Fig. 3, one can observe that the formulae using the HAM give more satisfactory results because the relative errors are relatively small. For the results from the formulae from the HAM, when the distance in the direction of the x-axis changes from 0 to 2 m, the errors become larger; however, when the distance changes from 2 to 4 m, the errors decrease with increasing distance. For the results at a large offset, the errors using the formulae from the perturbation analysis are larger than those from the HAM.

Exact series expansion coefficients

In this section, we have computed the coefficients of the series expansion. We use the same model size 4 km × 4 km as the last section but the source is located at (2 km, 10 m). Fig. 4 shows a colour plot of the coefficients of the traveltimes expansion in VTI media. Figs 4(a) and (b)

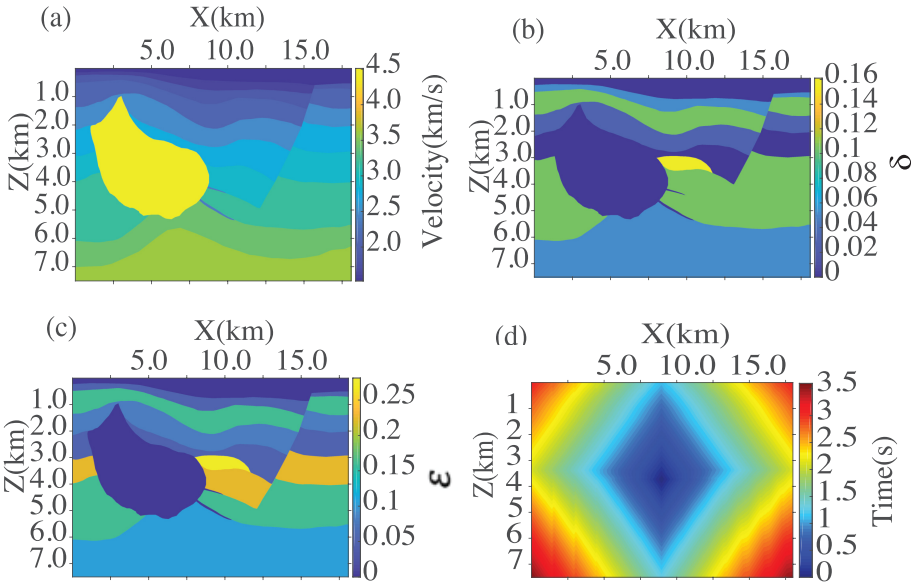

Figure 6. Colour plot of the traveltime using a modified Hess model with variable η. The size of the model is (18 km, 7.5 km). The source is located at the centre of the model (9 km, 3.75 km). Plot (a) shows velocity model, plot (b) shows δ model, plot (c) shows η model and plot (d) shows the traveltime.

show the results of the first-order coefficients and Figs 4(c) and (d) show the results of the second-order coefficients. The elastic parameters are $C_{11} = 25.7$, $C_{13} = 15.2$, $C_{33} = 15.4$, $C_{44} = 4.2$, $C_{66} = 9.0$ ($\eta = 0.16$, $\varepsilon = 0.33$ and $\delta = 0.81$) for (a) and (c), and $C_{11} = 35.7$, $C_{13} = 17.2$, $C_{33} = 15.4$, $C_{44} = 4.2$, $C_{66} = 9.0$ ($\eta = 0.1$, $\varepsilon = 0.66$ and $\delta = 0.92$) for (b) and (d). From Fig. 4, differences between the first-order coefficients and the second-order coefficients are notable. Whereas for the first-order coefficients, the large values are concentrated in the region along the vertical direction from the source, the values of the second-order coefficients are relatively large near the boundaries on both sides of the model. However, there is some similarity in shape between the first-order coefficients and the second-order coefficients, which shows similar effects of the coefficients on the traveltimes in VTI media.

Effects of anisotropic parameters

Finally, we perform numerical tests to analyse the effects of the anisotropic parameters on the traveltimes. The size of the model is 4 km × 4 km and the source is located at (2 km, 10 m). The NMO velocity is 2 km s^{-1} and the anisotropic parameters are $\eta = 0.2$ and $\delta = 0.2$, respectively. Figs 5(a) and (c) show colour plots of the traveltimes at a fixed location of (1 km, 1 km). Figs 5(b) and (d) show the colour plots of the traveltimes at a fixed location of (2.5 km, 4.0 km). From Fig. 5, one can observe that there are some common features: (1) whether using the HAM or the perturbation theory, there are more substantial effects on the traveltimes with an increasing anisotropic parameter η; (2) the maximum values for both methods occur in the region where the values of the anisotropic parameters η and δ are maximal. As for the locations of (1 km, 1 km) and (2.5 km, 4.0 km), the images are similar. As expected, the effects increase as the anisotropic parameters increase.

All the numerical tests so far have been based on the constant η. In real cases, however, η will be variable. One of the advantages of the approach is to deal with the variable η. We computed the traveltime in the Hess VTI model with variable η. Fig. 6 shows a colour plot of the traveltime using a modified Hess model with variable η. The size of the model is (18 km, 7.5 km). The source is located at the centre of the model (9 km, 3.75 km). Plot (a) shows the velocity model, plot (b) shows the δ model, plot (c) shows the η model and plot (d) shows the traveltime.

DISCUSSION AND CONCLUSION

We have presented a methodology and formulations for retrieving the eikonal equations for VTI and TTI media. The main advantage of the new HAM formulation in this paper is that it can be used for strongly anisotropic media. The formulation involves the initial approximation for the traveltimes, which is given by an analytical formulation or estimated by a numerical method. The derived linear equations involve the anisotropic parameters. We have derived the traveltime approximations for computing the traveltimes in VTI and TTI media using the HAM. We have demonstrated that the traveltime approximations based on the HAM can be used for computing the traveltimes in strongly anisotropic media. A comparison between traveltime approximations from the HAM and the perturbation theory has been carried out which shows that in strongly anisotropic media, the former has a higher accuracy. Finally, we have shown the effects of the coefficients of the series

solutions and the anisotropic parameters on the traveltimes. Because the HAM does not rely on the small perturbation assumption, we think that it is promising for applications to geophysical problems, for example, renormalization of scattering series.

ACKNOWLEDGEMENTS

XH acknowledges the Research Council of Norway for the Petromaks II project 267769/E3 (Bayesian inversion of 4D seismic waveform data for quantitative integration with production data). The authors are greatly grateful to Einar Iversen for insightful suggestions and valuable discussions. Some of the work was performed when XH had a visit from the University of Bergen to work for his PhD project at the University of California, Santa Cruz. We would like to thank the editor, Herve Chauris, the reviewer Tariq Alkhalifah and an anonymous reviewer for their insightful and constructive comments on the manuscript.

REFERENCES

Alkhalifah, T., 2000. An acoustic wave equation for anisotropic media, *Geophysics,* **65**(4), 1239–1250.

Alkhalifah, T., 2011a. Scanning anisotropy parameters in complex media, *Geophysics,* **76**(2), U13–U22.

Alkhalifah, T., 2011b. Traveltime approximations for transversely isotropic media with an inhomogeneous background, *Geophysics,* **76**(3), WA31–WA42.

Alkhalifah, T., 2013. Traveltime approximations for inhomogeneous transversely isotropic media with a horizontal symmetry axis, *Geophys. Prospect.,* **61**(3), 495–503.

Alkhalifah, T. & Choi, Y., 2014. From tomography to full-waveform inversion with a single objective function, *Geophysics,* **79**(2), R55–R61.

Alkhalifah, T. & Fomel, S., 2001. Implementing the fast marching eikonal solver: spherical versus cartesian coordinates, *Geophys. Prospect.,* **49**(2), 165–178.

Bai, C.-Y. & Greenhalgh, S., 2005. 3-D non-linear travel-time tomography: imaging high contrast velocity anomalies, *Pure appl. Geophys.,* **162**(11), 2029–2049.

Bai, C.-Y., Greenhalgh, S. & Zhou, B., 2007. 3D ray tracing using a modified shortest-path method, *Geophysics,* **72**(4), T27–T36.

Bouteiller, L.P., Benjemaa, M., Métivier, L. & Virieux, J., 2017. An accurate discontinuous galerkin method for solving point-source eikonal equation in 2-D heterogeneous anisotropic media, *Geophys. J. Int.,* **212**(3), 1498–1522.

Cao, S. & Greenhalgh, S., 1994. Finite-difference solution of the eikonal equation using an efficient, first-arrival, wavefront tracking scheme, *Geophysics,* **59**(4), 632–643.

Chapman, C.T. & Pratt, R., 1992. Traveltime tomography in anisotropic media I. Theory, *Geophys. J. Int.,* **109**(1), 1–19.

Crampin, S., 1984. Effective anisotropic elastic constants for wave propagation through cracked solids, *Geophys. J. Int.,* **76**(1), 135–145.

Červenỳ, V., 1972. Seismic rays and ray intensities in inhomogeneous anisotropic media, *Geophys. J. R. astr. Soc.,* **29**(1), 1–13.

Ĉervenŷ, V., 2001. *Seismic Ray Theory,* Cambridge Univ. Press.

Červenỳ, V. & Pšenčík, I., 1983. Gaussian beams in two-dimensional elastic inhomogeneous media, *Geophys. J. Int.,* **72**(2), 417–433.

Červenỳ, V., Klimeš, L. & Pšenčík, I., 2007. Seismic ray method: recent developments, *Adv. Geophys.,* **48,** 1–126.

Červenỳ, V., Iversen, E. & Pšenčík, I., 2012. Two-point paraxial traveltimes in an inhomogeneous anisotropic medium, *Geophys. J. Int.,* **189**(3), 1597–1610.

Farra, V. & Pšenčík, I., 2017. Weak-anisotropy moveout approximations for P-waves in homogeneous TOR layers, *Geophysics,* **82**(4), WA23–WA32.

Han, S., Zhang, W. & Zhang, J., 2017. Calculating qP-wave traveltimes in 2-D TTI media by high-order fast sweeping methods with a numerical quartic equation solver, *Geophys. J. Int.,* **210**(3), 1560–1569.

Hao, Q. & Alkhalifah, T., 2017. An acoustic eikonal equation for attenuating transversely isotropic media with a vertical symmetry axis, *Geophysics,* **82**(1), C9–C20.

Huang, X. & Greenhalgh, S., 2018. Linearized formulations and approximate solutions for the complex eikonal equation in orthorhombic media and applications of complex seismic traveltime, *Geophysics,* **83**(3), C115–C136.

Huang, X. & Sun, H., 2018. Numerical modeling of Gaussian beam propagation and diffraction in inhomogeneous media based on the complex eikonal equation, *Acta Geophys.,* **66**(4), 497–508.

Huang, X., Sun, H. & Sun, J., 2016a. Born modeling for heterogeneous media using the Gaussian beam summation based Green's function, *J. appl. Geophys.,* **131,** 191–201.

Huang, X., Sun, J. & Sun, Z., 2016b. Local algorithm for computing complex travel time based on the complex eikonal equation, *Phys. Rev. E,* **93**(4), 1–10, doi:10.1103/PhysRevE.93.043307.

Huang, X., Sun, J. & Greenhalgh, S., 2018. On the solution of the complex eikonal equation in acoustic VTI media: a perturbation plus optimization scheme, *Geophys. J. Int.,* **214**(2), 907–932.

Iversen, E. & Tygel, M., 2008. Image-ray tracing for joint 3D seismic velocity estimation and time-to-depth conversion, *Geophysics,* **73**(3), S99–S114.

Liao, S., 1992a. Application of process analysis method to the solution of 2-D nonlinear progressive gravity waves, *J. Ship Res.,* **36,** 30–37.

Liao, S., 1992b. A second-order approximate analytical solution of a simple pendulum by the process analysis method, *J. Appl. Mech.,* **59**(4), 970–975.

Liao, S., 2003a. *Beyond Perturbation: Introduction to the Homotopy Analysis Method,* CRC Press.

Liao, S., 2012. *Homotopy Analysis Method in Nonlinear Differential Equations,* Springer.

Liao, S., Xu, D. & Stiassnie, M., 2016. On the steady-state nearly resonant waves, *J. Fluid Mech.,* **794,** 175–199.

Liao, S.J., 1992c. The proposed homotopy analysis technique for the solution of nonlinear problems, *PhD thesis*, Shanghai Jiao Tong University, Shanghai.

Liao, S.-J., 1999. A uniformly valid analytic solution of two-dimensional viscous flow over a semi-infinite flat plate, *J. Fluid Mech.,* **385,** 101–128.

Liao, S.-J., 2002. An analytic approximation of the drag coefficient for the viscous flow past a sphere, *Int. J. Non-Linear Mech.,* **37**(1), 1–18.

Liao, S.-J., 2003b. An analytic approximate technique for free oscillations of positively damped systems with algebraically decaying amplitude, *Int. J. Non-Linear Mech.,* **38**(8), 1173–1183.

Liao, S.-J., 2004. An analytic approximate approach for free oscillations of self-excited systems, *Int. J. Non-Linear Mech.,* **39**(2), 271–280.

Liao, S.-J., 2011. On the homotopy multiple-variable method and its applications in the interactions of nonlinear gravity waves, *Commun. Nonlinear Sci. Numer. Simul.,* **16**(3), 1274–1303.

Liao, S.-J. & Chwang, A., 1998. Application of homotopy analysis method in nonlinear oscillations, *J. Appl. Mech.,* **65**(4), 914–922.

Luo, S. & Qian, J., 2012. Fast sweeping methods for factored anisotropic eikonal equations: multiplicative and additive factors, *J. Sci. Comput.,* **52**(2), 360–382.

Masmoudi, N. & Alkhalifah, T., 2016. Traveltime approximations and parameter estimation for orthorhombic media, *Geophysics,* **81**(4), C127–C137.

Moser, T., 1991. Shortest path calculation of seismic rays, *Geophysics,* **56**(1), 59–67.

Musgrave, M.J.P., 1970. *Crystal Acoustics: Introduction to the Study of Elastic Waves and Vibrations in Crystal,* Holden-Day.

Noble, M., Gesret, A. & Belayouni, N., 2014. Accurate 3-D finite difference computation of traveltimes in strongly heterogeneous media, *Geophys. J. Int.,* **199**(3), 1572–1585.

Pšenčík, I. & Farra, V., 2017. Reflection moveout approximations for P-waves in a moderately anisotropic homogeneous tilted transverse isotropy layer, *Geophysics,* **82**(5), C175–C185.
Rawlinson, N. & Sambridge, M., 2004a. Multiple reflection and transmission phases in complex layered media using a multistage fast marching method, *Geophysics,* **69**(5), 1338–1350.
Rawlinson, N. & Sambridge, M., 2004b. Wave front evolution in strongly heterogeneous layered media using the fast marching method, *Geophys. J. Int.,* **156**(3), 631–647.
Schoenberg, M., 1983. Reflection of elastic waves from periodically stratified media with interfacial slip, *Geophys. Prospect.,* **31**(2), 265–292.
Sethian, J.A., 1996. A fast marching level set method for monotonically advancing fronts, *Proc. Natl. Acad. Sci. USA,* **93**(4), 1591–1595.
Sethian, J.A. & Popovici, A.M., 1999. 3-D traveltime computation using the fast marching method, *Geophysics,* **64**(2), 516–523.
Silva, N.V.D., Ratcliffe, A., Vinje, V. & Conroy, G., 2016. A new parameter set for anisotropic multiparameter full-waveform inversion and application to a north sea data set, *Geophysics,* **81**(4), U25–U38.
Stovas, A. & Alkhalifah, T., 2012. A new traveltime approximation for TI media, *Geophysics,* **77**(4), C37–C42.
Stovas, A., Masmoudi, N. & Alkhalifah, T., 2016. Application of perturbation theory to a P-wave eikonal equation in orthorhombic media eikonal equation in orthorhombic media, *Geophysics,* **81**(6), C309–C317.
Tsvankin, I., 1997. Anisotropic parameters and P-wave velocity for orthorhombic media, *Geophysics,* **62**(4), 1292–1309.
Tsvankin, I., 2012. *Seismic Signatures and Analysis of Reflection Data in Anisotropic Media,* Society of Exploration Geophysicists.
Vidale, J., 1988. Finite-difference calculation of travel times, *Bull. seism. Soc. Am.,* **78**(6), 2062–2076.
Vinje, V., Iversen, E. & Gjøystdal, H., 1993. Traveltime and amplitude estimation using wavefront construction, *Geophysics,* **58**(8), 1157–1166.
Waheed, U.B. & Alkhalifah, T., 2017. A fast sweeping algorithm for accurate solution of the tilted transversely isotropic eikonal equation using factorization, *Geophysics,* **82**(6), WB1–WB8.
Waheed, U.B., Alkhalifah, T. & Stovas, A., 2013. Diffraction traveltime approximation for TI media with an inhomogeneous background, *Geophysics,* **78**(5), WC103–WC111.
Waheed, B.U., Yarman, C.E. & Flagg, G., 2015a. An iterative, fast-sweeping-based eikonal solver for 3D tilted anisotropic media, *Geophysics,* **80**(3), C49–C58.
Waheed, U.B, Alkhalifah, T. & Wang, H., 2015b. Efficient traveltime solutions of the acoustic TI eikonal equation, *J. Comput. Phys.,* **282,** 62–76.
Wang, C., Zhu, J., Liao, S. & Pop, I., 2003. On the explicit analytic solution of Cheng–Chang equation, *Int. J. Heat Mass Transfer,* **46**(10), 1855–1860.
Xu, S., Stovas, A. & Hao, Q., 2017. Perturbation-based moveout approximations in anisotropic media, *Geophys. Prospect.,* **65**(5), 1218–1230.
Zelt, C.A. & Barton, P.J., 1998. Three-dimensional seismic refraction tomography: a comparison of two methods applied to data from the Faeroe basin, *J. geophys. Res.,* **103**(B4), 7187–7210.
Zhao, H., 2005. A fast sweeping method for eikonal equations, *Math. Comput.,* **74**(250), 603–627.
Zhou, B. & Greenhalgh, S., 2004. On the computation of elastic wave group velocities for a general anisotropic medium, *J. Geophys. Eng.,* **1**(3), 205–215.
Zhou, B., Greenhalgh, S. & Green, A., 2008. Nonlinear traveltime inversion scheme for crosshole seismic tomography in tilted transversely isotropic media, *Geophysics,* **73**(4), D17–D33.

APPENDIX: TRAVELTIME APPROXIMATION IN TTI MEDIA

In this appendix, we derive the traveltime approximations based on the HAM. Substituting eqs (31) into (22), we obtain

$$\tau_1 = \frac{1}{v^2v_t^2\left(x^2v_t^2+v^2z^2\right)^2}\left(\sqrt{\frac{x^2v_t^2+v^2z^2}{v^2v_t^2}}\left(-2\eta v^8z^4\sin^2\theta+2\eta v^8z^4\sin^2\theta\cos^2\theta+v^8z^4\left(-\sin^2\theta\right)\right.\right. \tag{A1}$$
$$v^6x^2z^2\left(-\sin^2\theta\right)v_t^2-2v^6xz^3\sin\theta\cos\theta v_t^2+v^6z^4v_t^2-v^6z^4\cos^2\theta v_t^2-2\eta v^6x^2z^2\sin^2\theta v_t^2-4\eta v^6$$
$$xz^3\sin\theta\cos\theta v_t^2+4\eta v^6xz^3\sin\theta\cos^3\theta v_t^2-4\eta v^6xz^3\sin^3\theta\cos\theta v_t^2-2v^4x^3z\sin\theta\cos\theta v_t^4+2v^4x^2z^2v_t^4$$
$$-2v^4x^2z^2\cos^2\theta v_t^4+2v^4xz^3\sin\theta\cos\theta v_t^4-4\eta v^4x^3z\sin\theta\cos\theta v_t^4-2\eta v^4x^2z^2\cos^2\theta v_t^4+2\eta v^4x^2z^2$$
$$\cos^4\theta v_t^4-8\eta v^4x^2z^2\sin^2\theta\cos^2\theta v_t^4+2\eta v^4x^2z^2\sin^4\theta v_t^4+v^2x^4v_t^6-v^2x^4\cos^2\theta v_t^6+2v^2x^3z\sin\theta$$
$$\cos\theta v_t^6v^2x^2z^2\sin^2\theta v_t^6-2\eta v^2x^4\cos^2\theta v_t^6-4\eta v^2x^3z\sin\theta\cos^3\theta v_t^6+4\eta v^2x^3z\sin^3\theta\cos\theta v_t^6-$$
$$\left.\left.2\eta x^4\sin^2\theta\cos^2\theta v_t^8+x^4\sin^2\theta v_t^8\right)+v^6z^4v_t^2+2v^4x^2z^2v_t^4+v^2x^4v_t^6\right)$$

and

$$\tau_2=\tau_{21}+\tau_{22}+\tau_{23}+\tau_{24}+\tau_{25}, \tag{A2}$$

where

$$\tau_{21} = 8\eta^2 v^{16} z^8 \sin^4\theta - 24\eta^2 v^{16} z^8 \sin^4\theta \cos^2\theta + 8\eta v^{16} z^8 \sin^4\theta - 12\eta v^{16} z^8 \sin^4\theta \cos^2\theta \quad \text{(A3)}$$
$$+2v^{16} z^8 \sin^4\theta + 16\eta^2 v^{16} z^8 \sin^4\theta \cos^4\theta + 8v^{14} x^2 z^6 \sin^4\theta v_t^2 - 3v^{14} z^8 \sin^2\theta v_t^2 + 8v^{14} z^8 \sin^2\theta$$
$$\cos^2\theta v_t^2 + 32\eta v^{14} x^2 z^6 \sin^4\theta v_t^2 - 44\eta v^{14} x^2 z^6 \sin^4\theta \cos^2\theta v_t^2 + 8\eta v^{14} x z^7 \sin^5\theta \cos\theta v_t^2$$
$$-6\eta v^{14} z^8 \sin^2\theta v_t^2 + 34\eta v^{14} z^8 \sin^2\theta \cos^2\theta v_t^2 - 28\eta v^{14} z^8 \sin^2\theta \cos^4\theta v_t^2 + 16\eta v^{14} z^8$$
$$\sin^4\theta \cos^2\theta v_t^2 + 32\eta^2 v^{14} x^2 z^6 \sin^4\theta v_t^2 - 88\eta^2 v^{14} x^2 z^6 \sin^4\cos^2\theta v_t^2 + 64\eta^2 v^{14} x^2 z^6 \sin^4\theta$$
$$\cos^4\theta v_t^2 + 16\eta^2 v^{14} x z^7 \sin^5\theta \cos\theta v_t^2 + 16\eta^2 v^{14} z^8 \sin^2\theta \cos^2\theta v_t^2 - 32\eta^2 v^{14} z^8 \sin^2\theta \cos^4\theta$$
$$v_t^2 + 16\eta^2 v^{14} z^8 \sin^2\theta \cos^6\theta v_t^2 + 32\eta^2 v^{14} z^8 \sin^4\theta \cos^2\theta v_t^2 - 32\eta^2 v^{14} z^8 \sin^4\theta \cos^4\theta v_t^2$$
$$+16\eta^2 v^{14} z^8 \sin^6\theta \cos^2\theta v_t^2 + 10v^{12} x^4 z^4 \sin^4\theta v_t^4 + 8v^{12} x^3 z^5 \sin^3\theta \cos\theta v_t^4 - 9v^{12} x^2 z^6 \sin^2\theta$$
$$v_t^4 + 20v^{12} x^2 z^6 \sin^2\theta \cos^2\theta v_t^4 - 6v^{12} x z^7 \sin\theta \cos\theta v_t^4 + 8v^{12} x z^7 \sin\theta \cos^3\theta v_t^4 + v^{12} z^8 v_t^4$$
$$-3v^{12} z^8 \cos^2\theta v_t^4 + 2v^{12} z^8 \cos^4\theta v_t^4 - 8v^{12} z^8 \sin^2\theta \cos^2\theta v_t^4 + 40\eta v^{12} x^4 z^4 \sin^4\theta v_t^4 - 32\eta$$
$$v^{12} x^4 z^4 \sin^4\theta \cos^2\theta v_t^4 + 32\eta v^{12} x^3 z^5 \sin^3\theta \cos\theta v_t^4 - 80\eta v^{12} x^3 z^5 \sin^3\theta \cos^3\theta v_t^4 + 56\eta$$
$$v^{12} x^3 z^5 \sin^5\theta \cos\theta v_t^4 - 18\eta v^{12} x^2 z^6 \sin^2\theta v_t^4 + 68\eta v^{12} x^2 z^6 \sin^2\theta \cos^2\theta v_t^4 - 20\eta v^{12} x^2 z^6$$
$$\sin^2\theta \cos^4\theta v_t^4 - 16\eta v^{12} x^2 z^6 \sin^4\theta \cos^2\theta v_t^4 + 4\eta v^{12} x^2 z^6 \sin^6\theta v_t^4 - 12\eta v^{12} x z^7 \sin\theta \cos\theta$$
$$v_t^4 + 52\eta v^{12} x z^7 \sin\theta \cos^3\theta v_t^4 - 40\eta v^{12} x z^7 \sin\theta \cos^5\theta v_t^4 - 20\eta v^{12} x z^7 \sin^3\theta \cos\theta v_t^4 + 80\eta v^{12}$$
$$x z^7 \sin^3\theta \cos^3\theta v_t^4 - 16\eta v^{12} x z^7 \sin^5\theta \cos\theta v_t^4 - 16\eta v^{12} z^8 \sin^2\theta \cos^2\theta v_t^4 + 16\eta v^{12} z^8 \sin^2\theta$$
$$\cos^4\theta v_t^4 - 16\eta v^{12} z^8 \sin^4\theta \cos^2\theta v_t^4 + 40\eta^2 v^{12} x^4 z^4 \sin^4\theta v_t^4 - 64\eta^2 v^{12} x^4 z^4 \sin^4\theta \cos^2\theta v_t^4$$
$$+32\eta^2 v^{12} x^3 z^5 \sin^3\theta \cos\theta v_t^4 - 160\eta^2 v^{12} x^3 z^5 \sin^3\theta \cos^3\theta v_t^4 + 192\eta^2 v^{12} x^3 z^5 \sin^3\theta \cos^5\theta$$
$$v_t^4 + 112\eta^2 v^{12} x^3 z^5 \sin^5\theta \cos\theta v_t^4 - 192\eta^2 v^{12} x^3 z^5 \sin^5\theta \cos^3\theta v_t^4 + 16\eta^2 v^{12} x^2 z^6 \sin^2\theta \cos^2\theta$$
$$v_t^4 + 48\eta^2 v^{12} x^2 z^6 \sin^2\theta \cos^4\theta v_t^4 - 64\eta^2 v^{12} x^2 z^6 \sin^2\theta \cos^6\theta v_t^4 - 32\eta^2 v^{12} x^2 z^6,$$

$$\tau_{22} = \sin^4\theta \cos^2\theta v_t^4 + 192\eta^2 v^{12} x^2 z^6 \sin^4\theta \cos^4\theta v_t^4 + 8\eta^2 v^{12} x^2 z^6 \sin^6\theta v_t^4 - 64\eta^2 v^{12} x^2 z^6 \sin^6\theta \quad \text{(A4)}$$
$$\cos^2\theta v_t^4 + 32\eta^2 v^{12} x z^7 \sin\theta \cos^3\theta v_t^4 - 64\eta^2 v^{12} x z^7 \sin\theta \cos^5\theta v_t^4 + 32\eta^2 v^{12} x z^7 \sin\theta \cos^7\theta v_t^4$$
$$+160\eta^2 v^{12} x z^7 \sin^3\theta \cos^3\theta v_t^4 - 160\eta^2 v^{12} x z^7 \sin^3\theta \cos^5\theta v_t^4 - 32\eta^2 v^{12} x z^7 \sin^5\theta \cos\theta v_t^4$$
$$+160\eta^2 v^{12} x z^7 \sin^5\theta \cos^3\theta v_t^4 - 32\eta^2 v^{12} x z^7 \sin^7\theta \cos\theta v_t^4 + 4v^{10} x^6 z^2 \sin^4\theta v_t^6 + 16v^{10} x^5 z^3$$
$$\sin^3\theta \cos\theta v_t^6 - 9v^{10} x^4 z^4 \sin^2\theta v_t^6 + 20v^{10} x^4 z^4 \sin^2\theta \cos^2\theta v_t^6 - 18v^{10} x^3 z^5 \sin\theta \cos\theta v_t^6 + 24v^{10}$$
$$x^3 z^5 \sin\theta \cos^3\theta v_t^6 - 8v^{10} x^3 z^5 \sin^3\theta \cos\theta v_t^6 + 4v^{10} x^2 z^6 v_t^6 - 12v^{10} x^2 z^6 \cos^2\theta v_t^6 + 8v^{10} x^2 z^6$$
$$\cos^4\theta v_t^6 - 16v^{10} x^2 z^6 \sin^2\theta \cos^2\theta v_t^6 - 4v^{10} x^2 z^6 \sin^4\theta v_t^6 + 6v^{10} x z^7 \sin\theta \cos\theta v_t^6 - 8v^{10} x z^7$$
$$\sin\theta \cos^3\theta v_t^6 + 8v^{10} x z^7 \sin^3\theta \cos\theta v_t^6 + 4v^{10} z^8 \sin^2\theta \cos^2\theta v_t^6 + 16\eta v^{10} x^6 z^2 \sin^4\theta v_t^6$$
$$+64\eta v^{10} x^5 z^3 \sin^3\theta \cos\theta v_t^6 - 80\eta v^{10} x^5 z^3 \sin^3\theta \cos^3\theta v_t^6 + 48\eta v^{10} x^5 z^3 \sin^5 \cos v_t^6 - 18\eta v^{10}$$
$$x^4 z^4 \sin^2 v_t^6 + 50\eta v^{10} x^4 z^4 \sin^2 \cos^2 v_t^6 - 56\eta v^{10} x^4 z^4 \sin^2 \cos^4 v_t^6 + 80\eta v^{10} x^4 z^4 \sin^4\theta \cos^2\theta v_t^6$$
$$-12\eta v^{10} x^4 z^4 \sin^6\theta v_t^6 - 36\eta v^{10} x^3 z^5 \sin\theta \cos\theta v_t^6 + 120\eta v^{10} x^3 z^5 \sin\theta \cos^3\theta v_t^6 - 56\eta v^{10} x^3$$
$$z^5 \sin\theta \cos^5\theta v_t^6 - 56\eta v^{10} x^3 z^5 \sin^3\theta \cos\theta v_t^6 + 80\eta v^{10} x^3 z^5 \sin^3\theta \cos^3\theta v_t^6 + 16\eta v^{10} x^3 z^5$$
$$\sin^5\theta \cos\theta v_t^6 - 6\eta v^{10} x^2 z^6 \cos^2\theta v_t^6 + 18\eta v^{10} x^2 z^6 \cos^4\theta v_t^6 - 12\eta v^{10} x^2 z^6 \cos^6\theta v_t^6 - 72\eta$$
$$v^{10} x^2 z^6 \sin^2\theta \cos^2\theta v_t^6 + 96\eta v^{10} x^2 z^6 \sin^2\theta \cos^4\theta v_t^6 + 2\eta v^{10} x^2 z^6 \sin^4\theta v_t^6 - 40\eta v^{10} x^2$$
$$z^6 \sin^4\theta \cos^2\theta v_t^6 - 16\eta v^{10} x z^7 \sin\theta \cos^3\theta v_t^6 + 16\eta v^{10} x z^7 \sin\theta \cos^5\theta v_t^6 + 16\eta v^{10} x z^7$$
$$\sin^3\theta \cos\theta v_t^6 - 80\eta v^{10} x z^7 \sin^3\theta \cos^3\theta v_t^6 + 32\eta v^{10} x z^7 \sin^5\theta \cos\theta v_t^6 + 16\eta^2 v^{10} x^6 z^2$$
$$\sin^4\theta v_t^6 + 64\eta^2 v^{10} x^5 z^3 \sin^3\theta \cos\theta v_t^6 - 160\eta^2 v^{10} x^5 z^3 \sin^3\theta \cos^3\theta v_t^6 + 96\eta^2 v^{10} x^5 z^3$$
$$\sin^5\theta \cos\theta v_t^6 - 48\eta^2 v^{10} x^4 z^4 \sin^2\theta \cos^4\theta v_t^6 + 208\eta^2 v^{10} x^4 z^4 \sin^2\theta \cos^6\theta v_t^6 + 160\eta^2$$
$$v^{10} x^4 z^4 \sin^4 \cos^2\theta\theta v_t^6,$$

$$\tau_{23} = -544\eta^2 v^{10}x^4z^4\sin^4\theta\cos^4\theta v_t^6 - 24\eta^2 v^{10}x^4z^4\sin^6\theta v_t^6 + 208\eta^2 v^{10}x^4z^4\sin^6\theta\cos^2\theta v_t^6 + 64\eta^2 v^{10}x^3z^5\sin\theta\cos^3\theta v_t^6 - 64\eta^2 v^{10}x^3z^5\sin\theta\cos^7\theta v_t^6 + 448\eta^2 v^{10}x^3z^5\sin^3\theta\cos^5\theta v_t^6 + 32\eta^2 v^{10}x^3z^5\sin^5\theta\cos\theta v_t^6 - 448\eta^2 v^{10}x^3z^5\sin^5\theta\cos^3\theta v_t^6 + 64\eta^2 v^{10}x^3z^5\sin^7\theta\cos\theta v_t^6 + 16\eta^2 v^{10}x^2z^6\cos^4\theta v_t^6 - 32\eta^2 v^{10}x^2z^6\cos^6\theta v_t^6 + 16\eta^2 v^{10}x^2z^6\cos^8\theta v_t^6 + 224\eta^2 v^{10}x^2z^6\sin^2\theta\cos^4\theta v_t^6 - 224\eta^2 v^{10}x^2z^6\sin^2\theta\cos^6\theta v_t^6 - 128\eta^2 v^{10}x^2z^6\sin^4\theta\cos^2\theta v_t^6 + 480\eta^2 v^{10}x^2z^6\sin^4\theta\cos^4\theta v_t^6 - 224\eta^2 v^{10}x^2z^6\sin^6\theta\cos^2\theta v_t^6 + 16\eta^2 v^{10}x^2z^6\sin^8\theta v_t^6 + 8v^8x^7z\sin^3\theta\cos\theta v_t^8 - 3v^8x^6z^2\sin^2\theta v_t^8 + 12v^8x^6z^2\sin^2\theta\cos^2\theta v_t^8 - 18v^8x^5z^3\sin\theta\cos\theta v_t^8 + 24v^8x^5z^3\sin\theta\cos^3\theta v_t^8 - 16v^8x^5z^3\sin^3\theta\cos\theta v_t^8 + 6v^8x^4z^4v_t^8 - 18v^8x^4z^4\cos^2\theta v_t^8 + 12v^8x^4z^4\cos^4\theta v_t^8 - 16v^8x^4z^4\sin^2\theta\cos^2\theta v_t^8 - 8v^8x^4z^4\sin^4\theta v_t^8 + 18v^8x^3z^5\sin\theta\cos\theta v_t^8 - 24v^8x^3z^5\sin\theta\cos^3\theta v_t^8 + 16v^8x^3z^5\sin^3\theta\cos\theta v_t^8 - 3v^8x^2z^6\sin^2\theta v_t^8 + 12v^8x^2z^6\sin^2\theta\cos^2\theta v_t^8 - 8v^8xz^7\sin^3\theta\cos\theta v_t^8 + 32\eta v^8x^7z\sin^3\theta\cos\theta v_t^8 - 6\eta v^8x^6z^2\sin^2\theta v_t^8 + 32\eta v^8x^6z^2\sin^2\theta\cos^2\theta v_t^8 - 64\eta v^8x^6z^2\sin^2\theta\cos^4\theta v_t^8 + 112\eta v^8x^6z^2\sin^4\theta\cos^2\theta v_t^8 - 16\eta v^8x^6z^2\sin^6\theta v_t^8 - 36\eta v^8x^5z^3\sin\theta\cos\theta v_t^8 + 84\eta v^8x^5z^3\sin\theta\cos^3\theta v_t^8 - 32\eta v^8x^5z^3\sin\theta\cos^5\theta v_t^8 - 52\eta v^8x^5z^3\sin^3\theta\cos\theta v_t^8 + 80\eta v^8x^5z^3\sin^3\theta\cos^3\theta v_t^8 - 18\eta v^8x^4z^4\cos^2\theta v_t^8 + 44\eta v^8x^4z^4\cos^4\theta v_t^8 - 24\eta v^8x^4z^4\cos^6\theta v_t^8 - 112\eta v^8x^4z^4\sin^2\theta\cos^2\theta v_t^8 + 160\eta v^8x^4z^4\sin^2\theta\cos^4\theta v_t^8 + 4\eta v^8x^4z^4\sin^4\theta v_t^8 - 48\eta v^8x^4z^4\sin^4\theta\cos^2\theta v_t^8 - 52\eta v^8x^3z^5\sin\theta\cos^3\theta v_t^8 + 32\eta v^8x^3z^5\sin\theta\cos^5\theta v_t^8 + 52\eta v^8x^3z^5\sin^3\cos\theta v_t^8 - 80\eta v^8x^3z^5\sin^3\theta\cos^3\theta v_t^8 + 16\eta v^8x^2z^6\sin^2\theta\cos^2\theta v_t^8 - 64\eta v^8x^2z^6\sin^2\theta\cos^4\theta v_t^8 + 112\eta v^8x^2z^6\sin^4\theta\cos^2\theta v_t^8 - 16\eta v^8x^2z^6\sin^6\theta v_t^8 + 32\eta^2 v^8x^7z\sin^3\theta\cos\theta v_t^8 + 16\eta^2 v^8x^6z^2\sin^2\theta\cos^2\theta v_t^8 - 128\eta^2 v^8x^6z^2\sin^2\theta\cos^4\theta v_t^8 + 224\eta^2 v^8x^6z^2\sin^4\theta\cos^2\theta v_t^8 - 32\eta^2 v^8x^6z^2\sin^6\theta v_t^8 + 32\eta^2 v^8x^5z^3\sin\theta\cos^3\theta v_t^8 + 32\eta^2 v^8x^5z^3\sin\theta\cos^5\theta v_t^8 + 96\eta^2 v^8x^5z^3\sin\theta\cos^7\theta v_t^8 - 544\eta^2 v^8x^5z^3\sin^3\theta\cos^5\theta v_t^8 + 544\eta^2 v^8, \tag{A5}$$

$$\tau_{24} = x^5z^3\sin^5\theta\cos^3\theta v_t^8 - 96\eta^2 v^8x^5z^3\sin^7\theta\cos\theta v_t^8 + 40\eta^2 v^8x^4z^4\cos^4\theta v_t^8 - 24\eta^2 v^8x^4z^4\cos^6\theta v_t^8 - 16\eta^2 v^8x^4z^4\cos^8\theta v_t^8 + 160\eta^2 v^8x^4z^4\sin^2\theta\cos^4\theta v_t^8 + 320\eta^2 v^8x^4z^4\sin^2\theta\cos^6\theta v_t^8 - 48\eta^2 v^8x^4z^4\sin^4\theta\cos^2\theta v_t^8 - 768\eta^2 v^8x^4z^4\sin^4\theta\cos^4\theta v_t^8 + 320\eta^2 v^8x^4z^4\sin^6\theta\cos^2\theta v_t^8 - 16\eta^2 v^8x^4z^4\sin^8\theta v_t^8 + 96\eta^2 v^8x^3z^5\sin\theta\cos^5\theta v_t^8 - 96\eta^2 v^8x^3z^5\sin\theta\cos^7\theta v_t^8 - 160\eta^2 v^8x^3z^5\sin^3\theta\cos^3\theta v_t^8 + 544\eta^2 v^8x^3z^5\sin^3\theta\cos^5\theta v_t^8 - 544\eta^2 v^8x^3z^5\sin^5\theta\cos^3\theta v_t^8 + 96\eta^2 v^8x^3z^5\sin^7\theta\cos\theta v_t^8 + 4v^6x^8\sin^2\theta\cos^2\theta v_t^{10} - 6v^6x^7z\sin\theta\cos\theta v_t^{10} + 8v^6x^7z\sin\theta\cos^3\theta v_t^{10} - 8v^6x^7z\sin^3\theta\cos\theta v_t^{10} + 4v^6x^6z^2v_t^{10} - 12v^6x^6z^2\cos^2\theta v_t^{10} + 8v^6x^6z^2\cos^4\theta v_t^{10} - 16v^6x^6z^2\sin^2\theta\cos^2\theta v_t^{10} - 4v^6x^6z^2\sin^4\theta v_t^{10} + 18v^6x^5z^3\sin\theta\cos\theta v_t^{10} - 24v^6x^5z^3\sin\theta\cos^3\theta v_t^{10} + 8v^6x^5z^3\sin^3\theta\cos\theta v_t^{10} - 9v^6x^4z^4\sin^2\theta v_t^{10} + 20v^6x^4z^4\sin^2\theta\cos^2\theta v_t^{10} - 16v^6x^3z^5\sin^3\theta\cos\theta v_t^{10} + 4v^6x^2z^6\sin^4\theta v_t^{10} + 16\eta v^6x^8\sin^2\theta\cos^2\theta v_t^{10} - 12\eta v^6x^7z\sin\theta\cos\theta v_t^{10} + 16\eta v^6x^7z\sin\theta\cos^3\theta v_t^{10} - 16\eta v^6x^7z\sin\theta\cos^5\theta v_t^{10} - 16\eta v^6x^7z\sin^3\theta\cos\theta v_t^{10} + 80\eta v^6x^7z\sin^3\theta\cos^3\theta v_t^{10} - 32\eta v^6x^7z\sin^5\theta\cos\theta v_t^{10} - 18\eta v^6x^6z^2\cos^2\theta v_t^{10} + 34\eta v^6x^6z^2\cos^4\theta v_t^{10} - 12\eta v^6x^6z^2\cos^6\theta v_t^{10} - 72\eta v^6x^6z^2\sin^2\theta\cos^2\theta v_t^{10} + 96\eta v^6x^6z^2\sin^2\theta\cos^4\theta v_t^{10} + 2\eta v^6x^6z^2\sin^4\theta v_t^{10} - 40\eta v^6x^6z^2\sin^4\theta\cos^2\theta v_t^{10} - 56\eta v^6x^5z^3\sin\theta\cos^3\theta v_t^{10} + 56\eta v^6x^5z^3\sin\theta\cos^5\theta v_t^{10} + 56\eta v^6x^5z^3\sin^3\theta\cos\theta v_t^{10} - 80\eta v^6x^5z^3\sin^3\theta\cos^3\theta v_t^{10} - 16\eta v^6x^5z^3\sin^5\theta\cos\theta v_t^{10} + 50\eta v^6x^4z^4\sin^2\theta\cos^2\theta v_t^{10} - 56\eta v^6x^4z^4\sin^2\theta\cos^4\theta v_t^{10} + 80\eta v^6x^4z^4\sin^4\theta\cos^2\theta v_t^{10} - 12\eta v^6x^4z^4\sin^6\theta v_t^{10} + 80\eta v^6x^3z^5\sin^3\theta\cos^3\theta v_t^{10} - 48\eta v^6x^3z^5\sin^5\theta\cos\theta v_t^{10} + 16\eta^2 v^6x^8\sin^2\theta\cos^2\theta v_t^{10} - 32\eta^2 v^6x^7z\sin\theta\cos^5\theta v_t^{10} + 160\eta^2 v^6x^7z\sin^3\theta\cos^3\theta v_t^{10} - 64\eta^2 v^6x^7z\sin^5\theta\cos\theta v_t^{10} + 32\eta^2 v^6x^6z^2\cos^4\theta v_t^{10} + 8\eta^2 v^6x^6z^2\cos^6\theta v_t^{10} + 16\eta^2 v^6x^6z^2\cos^8\theta v_t^{10} - 32\eta^2 v^6x^6z^2\sin^2\theta\cos^4\theta v_t^{10} - 224\eta^2 v^6x^6z^2\sin^2\theta\cos^6\theta v_t^{10} + 48\eta^2 v^6x^6z^2\sin^4\theta\cos^2\theta v_t^{10} + 480\eta^2 v^6x^6z^2\sin^4\theta\cos^4\theta v_t^{10} - 224\eta^2 v^6x^6z^2\sin^6\theta\cos^2\theta v_t^{10} + 16\eta^2 v^6x^6z^2\sin^8\theta v_t^{10} + 112\eta^2 v^6x^5z^3\sin\theta\cos^5\theta v_t^{10} + 64\eta^2 v^6x^5z^3\sin\theta\cos^7\theta v_t^{10} - 160\eta^2 v^6x^5z^3\sin^3\theta\cos^3\theta v_t^{10} - 448\eta^2 v^6x^5z^3\sin^3\theta \tag{A6}$$

and

$$\tau_{25} = \Bigg(\cos^5\theta v_t^{10} + 448\eta^2 v^6 x^5 z^3 \sin^5\theta \cos^3\theta v_t^{10} - 64\eta^2 v^6 x^5 z^3 \sin^7\theta \cos\theta v_t^{10} - 64\eta^2 v^6 x^4 z^4 \sin^2\theta \cos^4\theta v_t^{10} \tag{A7}$$

$$+208\eta^2 v^6 x^4 z^4 \sin^2\theta \cos^6\theta v_t^{10} - 544\eta^2 v^6 x^4 z^4 \sin^4\theta \cos^4\theta v_t^{10} + 208\eta^2 v^6 x^4 z^4 \sin^6\theta \cos^2\theta v_t^{10} + v^4 x^8$$

$$v_t^{12} - 3v^4 x^8 \cos^2\theta v_t^{12} + 2v^4 x^8 \cos^4\theta v_t^{12} - 8v^4 x^8 \sin^2\theta \cos^2\theta v_t^{12} + 6v^4 x^7 z \sin\theta \cos\theta v_t^{12} - 8v^4 x^7 z$$

$$\sin\theta \cos^3\theta v_t^{12} - 9v^4 x^6 z^2 \sin^2\theta v_t^{12} + 20v^4 x^6 z^2 \sin^2\theta \cos^2\theta v_t^{12} - 8v^4 x^5 z^3 \sin^3\theta \cos\theta v_t^{12} + 10v^4 x^4 z^4$$

$$\sin^4\theta v_t^{12} - 6\eta v^4 x^8 \cos^2\theta v_t^{12} + 8\eta v^4 x^8 \cos^4\theta v_t^{12} - 16\eta v^4 x^8 \sin^2\theta \cos^2\theta v_t^{12} + 16\eta v^4 x^8 \sin^2\theta \cos^4\theta$$

$$v_t^{12} - 16\eta v^4 x^8 \sin^4\theta \cos^2\theta v_t^{12} - 20\eta v^4 x^7 z \sin\theta \cos^3\theta v_t^{12} + 40\eta v^4 x^7 z \sin\theta \cos^5\theta v_t^{12} + 20\eta v^4 x^7 z$$

$$\sin^3\theta \cos\theta v_t^{12} - 80\eta v^4 x^7 z \sin^3\theta \cos^3\theta v_t^{12} + 16\eta v^4 x^7 z \sin^5\theta \cos\theta v_t^{12} + 52\eta v^4 x^6 z^2 \sin^2\theta \cos^2\theta v_t^{12}$$

$$-20\eta v^4 x^6 z^2 \sin^2\theta \cos^4\theta v_t^{12} - 16\eta v^4 x^6 z^2 \sin^4\theta \cos^2\theta v_t^{12} + 4\eta v^4 x^6 z^2 \sin^6\theta v_t^{12} + 80\eta v^4 x^5 z^3 \sin^3\theta$$

$$\cos^3\theta v_t^{12} - 56\eta v^4 x^5 z^3 \sin^5\theta \cos\theta v_t^{12} - 32\eta v^4 x^4 z^4 \sin^4\theta \cos^2\theta v_t^{12} + 8\eta^2 v^4 x^8 \cos^4\theta v_t^{12} + 32\eta^2$$

$$v^4 x^8 \sin^2\theta \cos^4\theta v_t^{12} - 32\eta^2 v^4 x^8 \sin^4\theta \cos^2\theta v_t^{12} + 16\eta^2 v^4 x^7 z \sin\theta \cos^5\theta v_t^{12} - 32\eta^2 v^4 x^7 z \sin\theta$$

$$\cos^7\theta v_t^{12} + 160\eta^2 v^4 x^7 z \sin^3\theta \cos^5\theta v_t^{12} - 160\eta^2 v^4 x^7 z \sin^5\theta \cos^3\theta v_t^{12} + 32\eta^2 v^4 x^7 z \sin^7\theta \cos\theta v_t^{12}$$

$$-88\eta^2 v^4 x^6 z^2 \sin^2\theta \cos^4\theta v_t^{12} - 64\eta^2 v^4 x^6 z^2 \sin^2\theta \cos^6\theta v_t^{12} + 192\eta^2 v^4 x^6 z^2 \sin^4\theta \cos^4\theta v_t^{12} - 64$$

$$\eta^2 v^4 x^6 z^2 \sin^6\theta \cos^2\theta v_t^{12} - 192\eta^2 v^4 x^5 z^3 \sin^3\theta \cos^5\theta v_t^{12} + 192\eta^2 v^4 x^5 z^3 \sin^5\theta \cos^3\theta v_t^{12} - 3v^2$$

$$x^8 \sin^2\theta v_t^{14} + 8v^2 x^8 \sin^2\theta \cos^2\theta v_t^{14} + 8v^2 x^6 z^2 \sin^4\theta v_t^{14} + 18\eta v^2 x^8 \sin^2\theta \cos^2\theta v_t^{14} - 28\eta v^2 x^8$$

$$\sin^2\theta \cos^4\theta v_t^{14} + 16\eta v^2 x^8 \sin^4\theta \cos^2\theta v_t^{14} - 8\eta v^2 x^7 z \sin^5\theta \cos\theta v_t^{14} - 44\eta v^2 x^6 z^2 \sin^4\theta \cos^2\theta v_t^{14}$$

$$-24\eta^2 v^2 x^8 \sin^2\theta \cos^4\theta v_t^{14} + 16\eta^2 v^2 x^8 \sin^2\theta \cos^6\theta v_t^{14} - 32\eta^2 v^2 x^8 \sin^4\theta \cos^4\theta v_t^{14} + 16\eta^2 v^2 x^8$$

$$\sin^6\theta \cos^2\theta v_t^{14} + 64\eta^2 v^2 x^6 z^2 \sin^4\theta \cos^4\theta v_t^{14} + 2x^8 \sin^4\theta v_t^{16} - 12\eta x^8 \sin^4\theta \cos^2\theta v_t^{16} + 16\eta^2$$

$$x^8 \sin^4\theta \cos^4\theta v_t^{16} + \left(v^{12} z^6 v_t^6 + 3v^{10} x^2 z^4 v_t^8 + 3v^8 x^4 z^2 v_t^{10} + v^6 x^6 v_t^{12}\right) \sqrt{\frac{x^2 v_t^2 + v^2 z^2}{v^2 v_t^2}} \Bigg)$$

$$\Bigg/ \left(v^6 v_t^6 \left(x^2 v_t^2 + v^2 z^2\right)^3 \sqrt{\frac{x^2 v_t^2 + v^2 z^2}{v^2 v_t^2}} \right).$$